arXiv:0902.0814v2 [hep-ph] 19 Feb 2009

UCB-PTH-09/04

The Leptonic Higgs as a Messenger of Dark Matter

Hock-Seng Goh[1], Lawrence J. Hall[1,2], and Piyush Kumar[1]

[1] *Berkeley Center for Theoretical Physics, University of California, Berkeley, CA 94720 & Theoretical Physics Group, Lawrence Berkeley National Laboratory, Berkeley, CA 94720*

[2] *Institute for Physics and Mathematics of the Universe (IPMU) University of Tokyo, Kashiwa-no-ha 5-1-5, 277-8592, Japan.*

We propose that the leptonic cosmic ray signals seen by PAMELA and ATIC result from the annihilation or decay of dark matter particles via states of a leptonic Higgs doublet to τ leptons, linking cosmic ray signals of dark matter to LHC signals of the Higgs sector. The states of the leptonic Higgs doublet are lighter than about 200 GeV, yielding large $\bar{\tau}\tau$ and $\bar{\tau}\tau\bar{\tau}\tau$ event rates at the LHC. Simple models are given for the dark matter particle and its interactions with the leptonic Higgs, for cosmic ray signals arising from both annihilations and decays in the galactic halo. For the case of annihilations, cosmic photon and neutrino signals are on the verge of discovery.

Contents

I. Introduction 2

II. The Higgs as a Messenger of Dark Matter Signals 4

III. The Leptonic Higgs Boson 6

IV. Astrophysics Signals 9
A. Positrons (& Electrons) 10
B. Photons 14
C. Neutrinos 17

V. Higgs Physics - Collider Signals 19
A. The Higgs Potential 20
B. Potential Signals at the LHC 21
1. The $Z^* \to HA \to \bar{\tau}\tau\bar{\tau}\tau$ Signal 21
2. The $h, H \to \bar{\tau}\tau$ Signal 22
3. The $h \to HH, AA \to \bar{\tau}\tau\bar{\tau}\tau$ Signal 24

VI. Some simple DM Models with Leptonic Higgs 25
A. $L - L^c - N$ DM Model 25
1. Annihilating Dark Matter 26
2. Decaying Dark Matter 27
B. Singlet Scalar DM Model 28
C. Inert Higgs-Doublet DM Model 29

VII. Conclusions and Summary 30

Acknowledgments 32

References 32

I. INTRODUCTION

Recent observations of high-energy electron and positron cosmic ray spectra have generated tremendous interest, as they might provide the first non-gravitational evidence for Dark Matter (DM). The PAMELA [1] experiment reports an excess of positrons in the few GeV to 100 GeV range, providing further support to the earlier results of HEAT [2] and AMS [3]. In addition, results from the ATIC [4] and PPB-BETS [5] balloon experiments suggest an excess of electrons and positrons in the 300 GeV to 600 GeV range.

While these observations have conventional astrophysical interpretations, they may result from annihilations or decays of DM particles in the galactic halo. Indeed, the PAMELA and ATIC data reinforce each other, since, for a certain range of DM masses, they have a unified interpretation. However, DM

explanations for the leptonic cosmic ray excesses face two interesting challenges. First, for annihilating DM these signals require that the annihilation cross-section for DM particles is typically two to three orders of magnitude larger than that expected from the thermal freezeout of WIMP DM. On the other hand, for decaying DM, the life-time of the DM particles must be extremely large, of $\mathcal{O}(10^{25-26})$ seconds. Second, the signals apparently require annihilations or decays dominantly into leptons rather than hadrons, since there is no reported excess in anti-proton cosmic rays. Inspite of these challenges, many papers with different models of DM have already appeared in the literature, utilizing both annihilations [6, 7, 8, 9] and decays [10, 11, 12].

For annihilating DM, many of these models try to explain the required large annihilation cross-section by a Sommerfeld enhancement [13], which is operative at the non-relativistic velocities ($\beta \sim 10^{-3}$) in the galactic halo, while still having a standard thermal relic abundance applicable at the time of DM freeze-out. There are several possibilities for understanding why the products of the annihilation are dominantly leptonic rather than hadronic. One possibility is kinematics: the annihilation products of the DM particles are not heavy enough to decay into quarks, gauge bosons, and Higgs bosons, which have a large hadronic branching ratio, and hence decay only to electrons and muons (and possibly taus).

Another possibility is a *symmetry*, rather than kinematics, to understand why the DM annihilation or decay products are dominantly leptonic. In this work, we study a DM sector coupling to the visible sector through Higgs messengers which couple to leptons due to a symmetry. The plan of the paper is as follows. In the next section, we motivate this possibility from a general perspective, stressing that this is a natural implementation of the hypothesis that the DM is a WIMP, with mass and interactions broadly governed by the mass scale of weak interactions. In section III, we give the yukawa interactions for the minimal leptonic Higgs theory, and write them in a mass eigenstate basis for both the Higgs and the quarks and leptons. There are two Higgs scalars, h and H, one pseudoscalar, A, and one charged Higgs boson H^+, each with matter interactions that are determined by the ratio of vevs $\tan\beta$ and the Higgs mixing angle α. These interactions are quite unlike those of the usually considered two Higgs doublet model or of the MSSM. The LEP mass limits for h, H, A and H^+ are given, as well as constraints that follow from the cosmic ray signals.

In section IV the possible classes of DM annihilations and decays through the leptonic Higgs states H, A and H^+ are discussed. The common feature is multi-τ final states. For a particular annihilation channel the cosmic-ray electron and positrons signals are derived and compared to the PAMELA and ATIC data. In general, if the PAMELA and ATIC data result from enhanced galactic DM annihilation, then significant fluxes of photons [14, 15, 16] and neutrinos [17, 18] are also expected. On the one hand this could allow for a crucial confirmation of the DM nature of the signal, while on the other hand there is frequently some tension with present limits on photon and neutrino fluxes. We calculate photon fluxes in the leptonic Higgs model from DM annihilations in both the galactic center of the Milky Way and in the dwarf galaxy Sagittarius, and also discuss the neutrino flux.

In section V, we study the implications for Higgs signals at the LHC. The LHC Higgs signals are *necessarily correlated* with the cosmic-ray signals, with the leptonic Higgs states H, A and H^+ decaying dominantly to final states involving the τ lepton. The collider phenomenology is very rich, and quite unlike that of conventional two Higgs doublet models, such as the MSSM. In section VI, we study some simple models for the DM particle and its couplings to the Higgs sector, including the cases that the DM particle is derived from electroweak singlet and doublet fermions or scalars. Since our dark matter

particle is heavy, in the few TeV region, for DM annihilations the coupling strength to the leptonic Higgs is typically quite strong. In addition, a Sommerfeld enhancement of the annihilation cross section typically results from the exchange of the leptonic Higgs, which is lighter than $2M_W$. In the case of DM decays, the long lifetime results partly from the symmetry that forces one Higgs to be leptonic. We conclude in section VII.

II. THE HIGGS AS A MESSENGER OF DARK MATTER SIGNALS

FIG. 1: Three sectors and their interactions: the known quarks and leptons and their $SU(3) \times SU(2) \times U(1)$ gauge interactions, a Higgs sector and a WIMP Dark Matter sector.

What is our best guess for the structure of particle interactions at the TeV scale? In addition to the known physics of quarks and leptons interacting via $SU(3) \times SU(2) \times U(1)$ gauge interactions, we expect new physics to include both a Higgs sector, responsible for $SU(2) \times U(1)$ symmetry breaking, and a dark matter sector. While dark matter need not be related to the TeV scale, the WIMP idea is intriguing: if the dark matter particle mass is of order the TeV scale, the order of magnitude of the observed abundance results from thermal freezeout using simple dimensional analysis. Thus we are led to the three sectors of Figure 1: the known sector of quarks and leptons and their gauge interactions, together with the unknown sectors of the Higgs and WIMP dark matter.

What are the interactions between these sectors? Clearly the Higgs interacts directly with the quarks and leptons and $SU(2) \times U(1)$ gauge interactions, as shown, to give the observed masses. The interactions of the WIMP dark matter sector with the other two sectors are more speculative. In fact, there need not be any; the WIMP could annihilate to extremely light particles in its own sector. However, the WIMP idea is that the mass scales of the dark matter and Higgs sectors are related, and this strongly suggests some connection between these two sectors, as shown in Figure 1. Indeed, it could be that the Higgs and dark matter sectors are so closely connected that they merge. We assume that any direct couplings between the WIMP sector and the quark and lepton sector are subdominant, so that we are led to the pattern of connections of Figure 1. The Higgs sector is seen to be the messenger that makes the WIMP visible to us. The implications of this, for cosmic ray signatures of dark matter is clear. The WIMP, χ, will be observed via annihilations or decays through the Higgs particles. A simple realization of this idea is to introduce a singlet scalar to the SM, since the only gauge invariant renormalizable operator is a coupling to the Higgs [19]. This can be extended to supersymmetric theories by adding gauge singlet dark matter to the NMSSM [20].

What are the implications of the cosmic ray signals for this picture? The exciting thing is that the cosmic ray signals may shed light on the structure of the Higgs sector. The signals will depend on the nature and interactions of the Higgs states. The ATIC data suggests that the WIMP, χ, will be too

heavy to be observed at the LHC, so that the collider signals that could demonstrate consistency of the picture are those of the Higgs sector.

Could the Higgs sector simply be the single Higgs doublet of the Standard Model? Depending on its mass, the Higgs would decay dominantly to pairs of top quarks, W bosons, or bottom quarks. In either case, for any mass of the WIMP, the signal in $e^+ + e^-$ is smooth, and does not give the peak shown by the balloon experiments [21]. Hence the Standard Model Higgs can lead to the PAMELA positron signal, but not the ATIC $e^+ + e^-$ peak. If the latter is ignored, there is still the issue of whether dominant hadronic decays will produce a $\bar{p}$ flux larger than seen by PAMELA. For $m_\chi < 1$ TeV the $\bar{p}$ flux is apparenty one to two orders of magnitude too large. However, the uncertainties in the $\bar{p}$ signal are certainly an order of magnitude [22] and, by going to larger values of m_χ, the $\bar{p}$ spectrum can be shifted to larger energies where there is no data. For decays to top or bottom quark pairs, $m_\chi > 1$ TeV is in any case needed to explain the PAMELA signal. Values of m_χ around 100-200 GeV are possible for decays to W pairs, but this leads to some tension with data from anti-protons and gamma rays and also requires that the energy loss rate for positrons be larger [21, 23].

In this paper we concentrate on explanations of both the PAMELA e^+ data and the ATIC $e^+ + e^-$ peak. Quite generally this requires dominant cascades directly to charged leptons [21], so that we are immediately led to a Higgs that couples predominantly to leptons. Such Higgs bosons have received very little attention since they are not immediate consequences of either supersymmetric or grand unified theories (although this is possible with some model-building). For earlier work on Higgs bosons coupling to leptons with different motivation, see [24]. However, a leptonic higgs is the most straightforward implication of assuming that the cosmic ray data is explained by the annihilation or decay of WIMPs, χ, through Higgs messengers, as illustrated in Figure 1. Furthermore, the absence, to very high accuracy, of flavor violation in the charged lepton sector suggests that there is a single leptonic Higgs doublet, H_l. Thus, the experimental consequences for cosmic ray observations result from the connections below, while

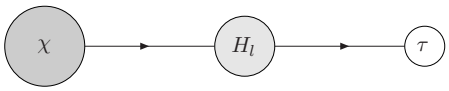

those for the LHC involve production of leptonic Higgs states followed by their decay to tau leptons.

The ATIC peak in the $e^+ + e^-$ channel will be broader than in theories where the signal results from χ cascading directly to e or μ. Also, there is the possibility of an energetic gamma-ray and neutrino component of the cosmic rays component in the energy range 100-1000 GeV. Both these signals could be detected in future experiments like GLAST/FERMI, VERITAS4 (gamma rays) and Hyper-Kamiokande, ANTARES, KM3neT, ICE-CUBE (neutrinos). These latter signals depend crucially on whether the cascade above results from the annihilation or decay of halo dark matter. We consider both possibilities in this paper.

Consider first the case that the cosmic ray signals arise from the annihilation of dark matter in the halo to H_l states. The size of the signal requires a galactic annihilation cross section that is significantly larger than the annihilation cross section required for a successful thermal freezeout abundance, so that a non-thermal production mechanism [25] is necessary. In the absence of thermal freeezeout one might wonder whether the motivation for WIMP dark matter is lost. Clearly the answer is no: the cosmic ray

signals have directly measured the annihilation cross section, and its order of magnitude is consistent with a weak scale mass – the WIMP motivation is actually strengthened.

On the other hand, if the cosmic ray signals result from decays of the dark matter in the halo, then the abundance of the dark matter could be given by the conventional thermal freezeout of WIMPs. New physics is now needed to induce a dark matter lifetime of order 10^{26} seconds. In the limit of stability, the theory possesses two discrete symmetries: one that prevents H_l from coupling to quarks and another that ensures the stability of χ. The decay chain $\chi \to H_l$ involves the breaking of both discrete symmetries. If the discrete symmetries are spontaneously broken at the weak scale v, then the dimensionless symmetry breaking parameters may be of order v/M, giving a χ decay rate of order $\Gamma_\chi \sim v^5/M^4$, which is the desired rate for $M \simeq 10^{16}$ GeV. While this is only a very rough order of magnitude estimate, it can be considered to be an extension of the WIMP idea, that the dark matter particle mass and interactions are governed by the weak scale.

In section VI we will introduce some explicit models for the dark matter sector and its coupling to the leptonic Higgs doublet. Each model can be considered in the "annihilation mode" or the "decay mode" depending on the absence or presence of the higher dimensional interactions that induce decay. Since these symmetry breaking effects are extremely small they will not affect the LHC signals of the model. Indeed, the main effect is on the size of the high energy photon and neutrino signals in the cosmic rays. For annihilations this depends on the square of the dark matter density, while for decays it is only linear in the density. The photon and neutrino signals have a much larger support from the center of the galaxy, or from satellite galaxies, while the lepton signal, because of propagation effects, has support from regions of the halo close to us. Thus it is likely to be the photon and neutrino signals that distinguish annihilations from decays. Moreover, as we will see, the neutrino signals tend to be more robust than the photon signals.

III. THE LEPTONIC HIGGS BOSON

Here we discuss the crucial features of the leptonic Higgs boson relevant for the PAMELA data; we postpone a discussion of the Higgs potential until section V. Consider a two Higgs doublet model with a symmetry that forces one Higgs doublet, H_l, to couple to the charged lepton sector and another, H_q, to couple to quarks

$$\mathcal{L}_{yuk} = y_u^{ij}\, Q_i\, u_j^c H_q^\dagger + y_d^{ij}\, Q_i\, d_j^c H_q + y_e^{ij}\, L_i\, e_j^c H_l + h.c. \tag{1}$$

where $Q_i, u_i^c, d_i^c, L_i, e_i^c$ are the quark and lepton fields with (i,j) being the family index, and $y_{u,d,e}^{ij}$ are the Yukawa coupling matrices.

We assume that the primary cosmic ray positron spectrum arises from cascade chains of the form

$$\chi(\chi) \to H(A) \to \bar\tau\tau(\bar\tau\tau) \to e^+ + \dots \tag{2}$$

where χ is some neutral dark matter particle, and H and A are a scalar and pseudoscalar of the Higgs sector, respectively. The chain could arise from either annihilation or decay of the dark matter particles, and the relative strength of the chains via H and A can vary. To suppress primary cosmic ray $\bar p$, H and A must lie dominantly in the leptonic Higgs doublet H_l. Writing the neutral component of the two Higgs

doublets as

$$H_l^0 = v_l + \frac{h_l + i a_l}{\sqrt{2}}, \qquad H_q^0 = v_q + \frac{h_q + i a_q}{\sqrt{2}}, \tag{3}$$

the H, A and h states may be written as

$$H = \cos\alpha\, h_l + \sin\alpha\, h_q; \qquad A = \cos\beta\, a_l - \sin\beta\, a_q; \qquad h = \sin\alpha\, h_l - \cos\alpha\, h_q \tag{4}$$

where

$$\tan\beta = \frac{v_l}{v_q} \ll 1; \qquad v_l^2 + v_q^2 = v^2 = (174\,\mathrm{GeV})^2 \tag{5}$$

and the mixing angle α, that diagonalizes the Higgs mass matrix, is also taken to be small,

$$\sin\alpha \ll 1. \tag{6}$$

While A is the only pseudoscalar, we call the scalar orthogonal to the higgs boson H as h. Since it lies dominantly in H_q, and since $v_q \gg v_l$, it is the scalar most closely related to electroweak symmetry breaking. It has many of the properties of the Standard Model Higgs boson, except that its couplings to leptons are not standard. Also, precision electroweak data do not require that m_h is close to the present experimental bound, since the other scalar states, and possibly the dark matter sector, may contribute to the S and T observables. In addition there is a charged scalar, H^+, that lies dominantly in H_l. The couplings of H, A, h and H^+ to quarks and leptons are proportional to the diagonal quark and lepton mass matrices, $m_{u,d,e}$:

$$\begin{aligned}
\mathcal{L}_H &= \frac{H}{\sqrt{2}v}\left(\frac{\sin\alpha}{\cos\beta}(u m_u u^c + d m_d d^c) + \frac{\cos\alpha}{\sin\beta}(e m_e e^c)\right) \\
\mathcal{L}_A &= \frac{iA}{\sqrt{2}v}\left(\frac{-\sin\beta}{\cos\beta}(u m_u u^c + d m_d d^c) + \frac{\cos\beta}{\sin\beta}(e m_e e^c)\right) \\
\mathcal{L}_h &= \frac{h}{\sqrt{2}v}\left(\frac{-\cos\alpha}{\cos\beta}(u m_u u^c + d m_d d^c) + \frac{\sin\alpha}{\sin\beta}(e m_e e^c)\right) \\
\mathcal{L}_{H^\pm} &= \frac{H^-}{v}\left(\frac{-\sin\beta}{\cos\beta}(u V_{CKM} m_d d^c + u^{c\dagger} m_u d^\dagger) + \frac{\cos\beta}{\sin\beta}(\nu_e m_e e^c)\right)
\end{aligned} \tag{7}$$

where V_{CKM} is the CKM mixing matrix of the charged current quark interaction.

The LEP experiments have placed bounds on the scalars H, A and H^+. The cross section for the process $e^+e^- \to ZH$ is proportional to $\sin^2(\alpha-\beta)$ and depends on m_H. The limits on $\sin^2(\alpha-\beta)$ are shown in Figure 2c of [26] for the case that H decays dominantly to $\bar\tau\tau$, as we expect. For $\sin(\alpha-\beta) = 0.3$ the H mass cannot lie in the region (30 - 100) GeV, but for $\sin(\alpha-\beta) < 0.2$ there is no limit. More importantly, the LEP experiments have searched for the process $e^+e^- \to HA$ which is proportional to $\cos^2(\alpha-\beta) \simeq 1$. In the case that both H and A decay dominantly to $\bar\tau\tau$ as we have, the limits are shown in Figure 4d of [26] and require that either $m_H + m_A < 20$ GeV, which is strongly excluded by the width of the Z boson, or

$$m_H + m_A > 185\,\mathrm{GeV}. \tag{8}$$

If the charged Higgs, H^+, is lighter than the tb and WZ thresholds, it will dominantly decay to $\tau\nu_\tau$, since the cs final state has a relative supression of $\tan^4\beta$. Thus the limit set by the ALEPH collaboration is [27]

$$m_{H^+} > 88\,\mathrm{GeV}. \tag{9}$$

In addition to these LEP constraints on the higgs masses, we require that the $H, A \to \bar{\tau}\tau$ branching ratios are dominant and at least 0.9. This is because the dark matter annihilation or decay chain passes through H/A states and we need to satisfy the $\bar{p}$ constraint from PAMELA. In particular to avoid final states involving electroweak gauge bosons we impose

$$|m_H - m_A| < m_Z \tag{10}$$

in order to suppress the mode $H \to A\,Z$ ($A \to H\,Z$), and

$$m_H < 2m_W. \tag{11}$$

to avoid $H \to 2W$. Finally, we require

$$m_H < 2\,m_A \tag{12}$$

in order to forbid the decay $H \to AA$ since such a cascade of H would lead to a less prominant peak in the lepton cosmic ray spectrum for ATIC. To summarize, these constraints impose limits on m_H and m_A:

$$\begin{aligned} \frac{2m_Z}{3} &< m_A < 2m_W + m_Z \\ \frac{m_Z}{2} &< m_H < 2m_W \end{aligned} \tag{13}$$

Under these conditions, H and A predominantly go to $\bar{\tau}\tau$. The decay to $b\bar{b}$ is suppressed due to the leptophilic nature of H and A.

How small should $\sin\alpha$ and $\sin\beta$ be taken in order that the H and A couplings to quarks are small enough to sufficiently suppress the $\bar{p}$ cosmic ray flux? For the mass range we are considering in this paper, the dominant decays are to $\bar{b}b$ and $\bar{\tau}\tau$. In this case, the ratio of quarks to leptons in the decays of H and A is

$$r_q^H = 3\,\frac{m_b^2}{m_\tau^2}\tan^2\alpha\tan^2\beta \tag{14}$$

and

$$r_q^A = 3\,\frac{m_b^2}{m_\tau^2}\tan^4\beta. \tag{15}$$

There is considerable uncertainty in the limit that the PAMELA $\bar{p}$ data imposes on r_q. For example, a limit of $r_q < 0.1$ can be satisfied by taking $\sin\alpha$ and $\sin\beta$ both $\lesssim 0.25$. The limits on the mixing angles become much more stringent for the case of heavier H and A, where decays to gauge boson or $\bar{t}t$ are possible. In this case, $\sin\alpha$ and $\sin\beta$ has to be sufficiently small. Although the required small mixing angles remain within acceptable value (the τ yukawa coupling does not become large), for simplicity and concreteness we will not consider this case for the rest of this paper.

IV. ASTROPHYSICS SIGNALS

DM particles in our galaxy and neighboring galaxies can annihilate or decay into Standard Model (SM) particles leading to production of cosmic rays such as electrons and positrons, protons and anti-protons, photons and neutrinos, which could be observed at the earth. Therefore, an observation of these cosmic rays consistent with DM annihilation or decay could serve as *indirect* detection of Dark Matter. However, a given framework for DM trying to explain a signal from one set of experiments must also respect bounds set from all other experiments.

In this section, we study the implications of the above framework for cosmic ray signals - positrons and photons in particular. We also make comments about implications for the cosmic neutrino flux from the Galactic Center (GC) at the end. In order to carry out the analysis, we make the assumption, motivated in the previous sections, that DM particles dominantly annihilate or decay into higgs particles which have dominant H_l components. This can be guaranteed by postulating a symmetry (either discrete or continuous)[1] and mass range for H and A given in the previous section.

We see that the robust and distinctive feature of the above framework is production of tau leptons which subsequently give rise to cosmic ray electrons and positrons, as well as photons and neutrinos. However, the precise signal for cosmic rays depends on model-dependent details. These can be broadly classified into five classes. For annihilating DM, be it bosonic or fermionic, one has the following:

$$\chi\chi \to HA\,(HH,\, AA) \to \bar{\tau}\tau\bar{\tau}\tau \tag{16}$$

For bosonic annihilating DM, it is also possible to have:

$$\chi\chi \to H^+H^- \to \bar{\tau}\tau\bar{\nu_\tau}\nu_\tau \tag{17}$$

whihc is forbidden at s-wave for a majorana fermion DM by CP conservation. On the other hand, for decaying DM, the signals for fermionic and bosonic DM are different. For bosonic DM, there are two possibilities:

$$\begin{aligned} \chi &\to HA(HH,\, AA) \to \bar{\tau}\tau\bar{\tau}\tau \\ \chi &\to \bar{\tau}\tau \end{aligned} \tag{18}$$

The second possibility in (18) can arise if the DM particle mixes with H or A which decays to $\bar{\tau}\tau$. Finally, for fermionic decaying DM, one has the possibilities:

$$\begin{aligned} \chi &\to H\,(A)\,\nu \to \bar{\tau}\tau\nu \\ \chi &\to H^{\mp}l^{\pm} \to \tau^{\mp}l^{\pm}\nu_\tau;\;\; l \equiv e, \mu, \tau \end{aligned} \tag{19}$$

In section VI, we will construct some simple models which exhibit all the above possibilities. Although a wide variety of signals for cosmic rays can arise within this framework, it is important to note that the annihilation and decay modes can be related. More precisely, for the same given state (for example, the 4 τ state in (16) and (18)), the signal for positrons and electrons in the annihilation mode for a DM

[1] Please see section VI for some explicit models.

particle with mass m_χ and cross-section $\langle\sigma\, v\rangle$ corresponds to that for a decaying DM particle with mass $2\, m_\chi$ and lifetime τ_χ given by:

$$\tau_\chi \approx \frac{m_\chi}{\rho_s \,\langle\sigma\, v\rangle} \tag{20}$$

where ρ_s is the dimensionful constant appearing in the DM profiles[2]. The above holds true to a very good approximation since the electrons and positrons observed at the earth come from a short distance in the galaxy[3] where differences in the various DM profiles are not important. Thus, the different dependence on the DM density profile ($\sim \rho$ for decays versus $\sim \rho^2$ for annihilations) does not have a big effect.

A. Positrons (& Electrons)

In this subsection, we will estimate the positron fraction (to be compared with PAMELA) and the total flux of electrons and positrons (to be compared with ATIC) as a function of the mass of the DM m_χ and that of the higgs particles m_H and m_A, consistent with the assumptions above. For concreteness, we will show the results for the annihilation channel (16) in which DM annihilates to 4 τ's via two intermediate higgs particles H, A. This can be easily translated to results for the first decay mode in (18) from arguments mentioned above. Similarly, results for the second decay mode in (18) can be translated from that obtained for the direct annihilation mode $\chi\chi \to \bar\tau\tau$ in [21]. We will review this result and also comment on the annihilation mode in (17) and the decay modes in (19) at the end of the subsection.

The cosmic-ray background of nuclei and electrons is believed to originate from supernovae remnants but is not fully understood. The nuclei and electron spectra is assumed to arise from an injected flux which follows a power law as a function of energy, and is then propagated through the galaxy within some "propagation models". In the course of propagation through the galactic medium, a secondary component of electrons and positrons is generated by spallation of the cosmic rays on the interstellar medium. The parameters of the source spectra and the propagation models are constrained by fitting to astrophysical data. For example, the nuclei source spectra and propagation parameters are constrained by fitting to the proton data, the Boron-to-Carbon (B/C) ratio and so on. Since background positrons are dominantly generated from spallation of nuclei, this constrains the background positron flux as well. The electron source spectra is mostly constrained from experiments measuring the total electron flux. Thus, in the absence of a complete theoretical understanding of the processes involving the production and propagation of these cosmic rays, there is a considerable amount of uncertainty in the background electron and positron flux arising both from uncertainties in the nuclei and electron source spectra, production cross-sections, energy losses, as well as those from parameters in the various propagation models. It turns out that the uncertainty in the background electron spectrum is larger than that in the propagation parameters at present. It is important to keep these facts in mind when one tries to explain the data observed by PAMELA and ATIC.

In addition to uncertainties in the background flux, there also exist uncertainties in the "signal" component assumed to arise from the annihilation or decay of DM particles. Once the injection spectrum

[2] For a given profile, ρ_s is constrained by requiring that $\rho_\chi(r = 8.5\,\mathrm{kpc}) \approx 0.3\,\mathrm{GeV/cm^3}$.
[3] more on this in section IV A.

of positrons at the source is specified, the primary positron flux $\Phi_{e^+}^{prim}$ at the solar system arising from DM annihilation in the Milky Way galactic halo is found by solving a diffusion equation (with cylindrical boundary conditions for a cylinder of half-height L=1-15 kpc and radius R=20 kpc) with a source function given by:

$$\begin{aligned} Q_{annih}^{e^+}(E', \vec{r'}) &= \frac{\rho_\chi^2(\vec{r'})}{2m_\chi^2} \langle \sigma\, v \rangle \frac{dN_{e^+}}{dE'}(E') \\ Q_{decay}^{e^+}(E', \vec{r'}) &= \frac{\rho_\chi(\vec{r'})}{m_\chi} \Gamma_\chi \frac{dN_{e^+}}{dE'}(E') \end{aligned} \tag{21}$$

where $\frac{dN_{e^+}}{dE'}(E')$ is the injection spectrum of positrons produced from DM annihilations or decay, and $\rho_\chi(\vec{r})$ is the density profile of DM in our Galaxy. As for the background, uncertainties exist in the propagation parameters. Some of the most important parameters include the half-height of the diffusion cylinder L, the parameters characterizing the diffusion process - $K = K_0\, \beta \mathcal{R}^\delta$, where K_0 is the diffusion constant, β is the velocity of the particle and $\mathcal{R}$ is its rigidity, defined as $\mathcal{R} = |\vec{p}\,(\mathrm{GeV})|/Z$ with Z as the atomic number, and the characteristic time for energy loss τ_E. Different sets of parameters $\{L, K_0, \delta\}$ exist which are consistent with astronomical data such as the B/C ratio, etc. The energy loss time τ_E has an uncertainty of about a factor of 2 [28]. The dependence on the DM profile is weak since the positrons come from a short distance ($\mathcal{O}$(1kpc)) where the different DM profiles are quite similar. However, the average local DM density, i.e. $\rho_\chi(r = 8.5\,\mathrm{kpc})$ is itself uncertain by a factor of 2 [29]. From (21), we see that this uncertainty can be accommodated by a simple rescaling of the cross-section (or decay width).

Keeping the above facts about the signal and background fluxes in mind, we have estimated the positron fraction and the total flux of electrons and positrons. For concreteness, we have used the parameters for the MED propagation model for the background and signal fluxes, as defined in [30]. The background electron spectral index α defined by $\Phi_{e^-}^{bkg} \sim E^{-\alpha}$ is taken to be 3.04, which is quite reasonable and is consistent with observations of all experiments [8]. The normalization of the background electron spectrum is determined by a similar procedure as described in [8]. Finally, we have used the Bessel approach to compute the Green's function of the diffusion equation. In particular, we have used an approximation to the Green's function found in [11] to solve the equation. The results of our analysis are shown in Figure 2.

We see from Figure 2 that the results for the positron fraction and the total electron and positron flux are sensitive to the mass of the DM m_χ as well as the "Boost factor" for electrons and positrons B_{tot}^e. The results are qualitatively consistent with that of [7] who have looked at a similar annihilation mode, although from a very different theoretical motivation and with much lighter masses of intermediate scalars. One finds that a DM particle with mass $m_\chi \sim$ TeV may explain the PAMELA data; however the explanation of *both* PAMELA and ATIC data requires that m_χ is about 4 TeV and $B_{tot}^e \approx 10000$. Also, it turns out that the above results have a mild dependence on the masses of the intermediate higgs particles m_H, m_A as long as 50 GeV $\lesssim m_H, m_A \lesssim$ few 100 GeV, which is the expected range of masses for H and A. Note that since the results depend on astrophysical parameters such as the electron spectral index α and the propagation model parameters as explained above, it is possible to fit the data for different (but comparable) values of m_χ and boost factors B_{tot}^e by choosing a different combination of these parameters. Also, if the ATIC data is ignored, the best fit values of the parameters m_χ and B_{tot}^e will be slightly different than when both data sets are taken into account. Hence, the above results

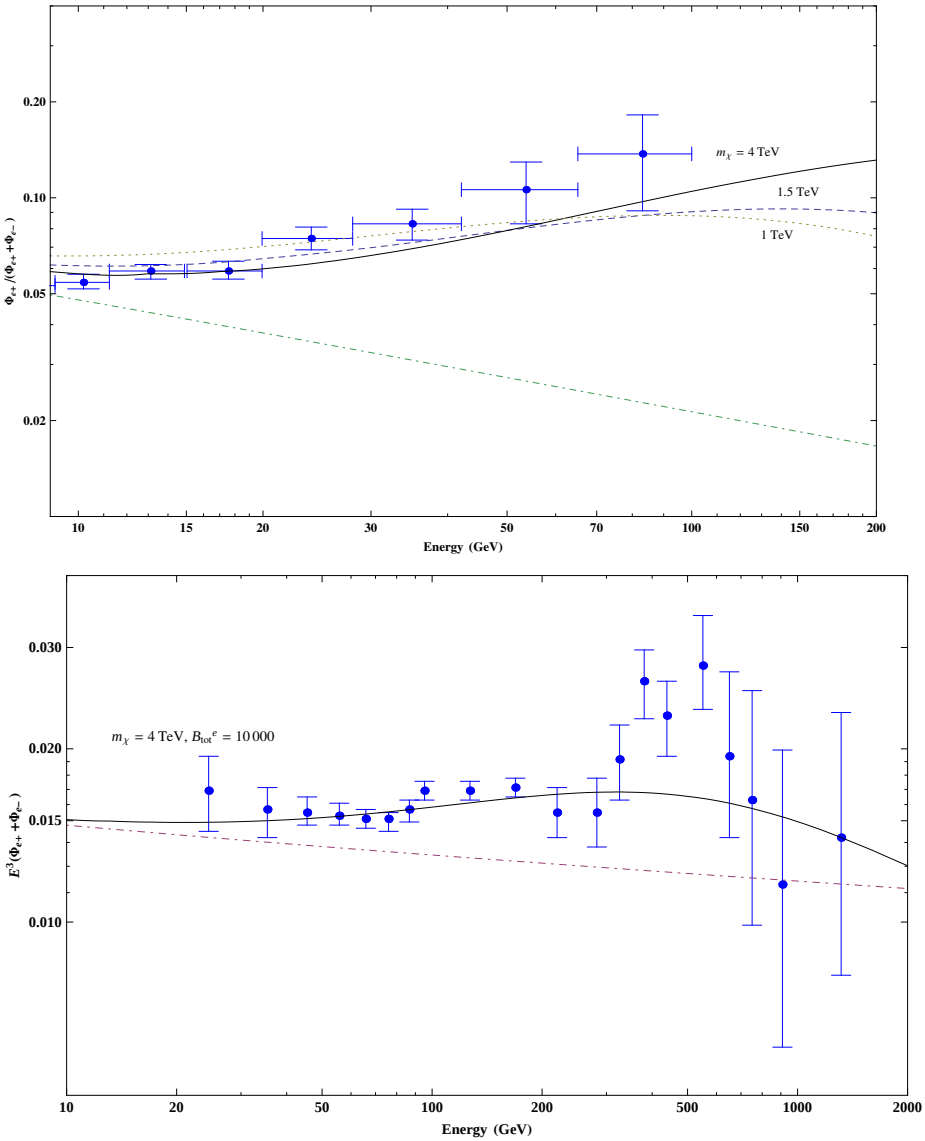

FIG. 2: Results for the positron fraction (**Top**) as a function of energy for DM masses $m_\chi = 1$ TeV (**dotted**), $m_\chi = 1.5$ TeV (**dashed**) and $m_\chi = 4$ TeV (**black**) and $m_H, m_A = 100$ GeV, in the annihilation mode (16) with "boost factors" B^e_{tot} given by 1200, 1950 and 10000 respectively. The result for $E^3(\Phi^{total}_{e^-} + \Phi^{total}_{e^+})$ (**Bottom**) as a function of energy is only shown for $m_\chi = 4$ TeV. The dot-dashed curve in both plots stands for the background. The background electron spectral index α is taken to be 3.04 and the MED propagation model [30] is used. Also, the reference values of the local DM density ρ_0 and τ_E are taken as 0.26 GeV/cm^3 and 10^{16} seconds respectively. The boost factor B^e_{tot} is explained below (22).

should only be taken as an estimate. We have not tried to optimize the fit (by a χ^2 analysis) by the choice of astrophysical parameters.

The boost factor B^e_{tot}, which is a combination of various factors, deserves some explanation. More precisely, the boost factor is given by:

$$B^e_{tot} = B_{\sigma v} \cdot B^e_{clump} \cdot B_{\rho_0} \cdot B_{\tau_E} \tag{22}$$

Here, $B^e_{\sigma v}$ is the enhancement factor in the cross-section compared to the "standard" one $\langle\sigma v\rangle_{std} = 3\times 10^{-26} cm^3/s$. B^e_{clump} corresponds to the enhancement in the positron (electron) signal due to clumpiness in the DM halo. Strictly speaking, B^e_{clump} is a function of energy [31]. Over the relevant energy range of 1-1000 GeV, B^e_{clump} of order few is reasonable. B_{ρ_0} is a possible enhancement due to a factor of two uncertainty in the local average DM density itself, as mentioned earlier. Note that a factor of two in ρ_0 appears as a factor of four in B_{ρ_0} because the flux goes as ρ_0^2. Finally, the factor of two uncertainty in the energy loss time τ_E mentioned above can be folded into a possible enhancement because the flux is directly proportional to τ_E. Thus, $B^e_{tot} \approx 10000$ can arise in many ways. In particular, it is perfectly compatible with $B_{\sigma v} \lesssim 1000$. In addition, the boost factor for neutrinos will in general be *different* than that for positrons (electrons). All these facts will be important when we look at constraints from photons and neutrinos in the following subsections as well as the section on explicit models in section VI.

Moving on to the other annihilation and decay modes, the energy spectra for τs and νs in the annihilation mode (17) is expected to be roughly the same as in (16) because m_τ and m_ν are both negligible compared to $m_{H^\pm}$. This suggests that it should be possible to fit the data for the same m_χ as for (16) but with twice the boost factor. However, due to $SU(2)$ invariance, we expect $\chi\chi \to AA,\ HH$ which gives rise to four τ, to also contribute with the same cross section. Taking the sum of these modes to be the total cross section and normalizing it to the standard thermal cross section, we need a factor of 4/3 relative to the B^e_{tot} required for only the four τ case. This implies $B^e_{tot} \approx 13300$ for $m_\chi \approx 4$ TeV.

As explained earlier, the results for the annihilation mode (16) can be translated to the first decay mode in (18). A DM mass of 4 TeV with $B^e_{tot} = 10000$ corresponds to decaying DM with $m_\chi = 8$ TeV and lifetime τ_χ given by [4]:

$$\tau_\chi \approx \frac{m_\chi}{2\,\rho_s\,\langle\sigma\,v\rangle_{std} B^e_{tot}} (\sqrt{B^e_{clump}\cdot B_{\rho_0}}\cdot B_{\tau_E}) \approx 3.2\times 10^{25}\,\mathrm{s}\,(\sqrt{B^e_{clump}\cdot B_{\rho_0}}\cdot B_{\tau_E}) \tag{23}$$

To get the results for the second decay mode in (18), one needs to translate the results obtained for the direct annihilation mode $\chi\chi \to \tau\tau$ in [21]. From [21], one finds that the $\chi\chi \to \tau\tau$ mode gives a good fit to the PAMELA and ATIC data for $m_\chi \approx 2$ TeV and $B^e_{tot} \approx 3000$. This corresponds, for the second decay mode in (18), to $m_\chi = 4$ TeV and lifetime τ_χ given by:

$$\tau_\chi \approx 5.3\times 10^{25}\,\mathrm{s}\,(\sqrt{B^e_{clump}\cdot B_{\rho_0}}\cdot B_{\tau_E}) \tag{24}$$

Finally, we comment on the fermionic DM decay modes in (19). [11] studied the first decay mode in (19) and found that m_χ between 600 GeV and 1 TeV can explain the PAMELA data. It was pointed out in [12] that this decay mode can also provide a good fit to both PAMELA and ATIC. The second decay mode in (19) is qualitatively different, since the lepton l is harder than the τ. For $l = e, \mu$ this provides a contribution to the spectrum which is steeper than that coming from the τ, implying that it should be possible to fit the data with a lighter m_χ and a smaller boost factor.

To summarize, therefore, even though the precise signal for astrophysics depends on model-dependent details, the robust characteristic of the framework is that an annihilating (decaying) DM particle with mass of 4 (2-8) TeV and $B^e_{tot} = O(10000 - 13000)$ ($\tau_\chi = 10^{25-26}$ s) can explain the PAMELA and ATIC

[4] $\sqrt{B_{\rho_0}}$ arises due to the fact that the flux goes as ρ_0^2 for annihilations but as ρ_0 for decays.

results. We now study the consequences for cosmic gamma rays and neutrinos which provide non-trivial constraints on the allowed parameter space as well as give rise to potential signals for future experiments.

B. Photons

In general, any model of DM which produces a significant number of electrons and positrons in the local region of our galaxy in the energy range 10-1000 GeV (to explain the PAMELA and ATIC signals), is expected to dominate the production of electrons and positrons in the galactic center (GC) since the density of DM is expected to be much larger there. This will in turn give rise to a large yield of photons from inverse compton scattering (ICS) in the energy range 1-1000 GeV. In addition, there could be other mechanisms of photon production from DM annhilations or decays, such as final-state radiation (FSR) of photons from charged particle production, DM Bremsstrahlung, or from π^0s produced from τ decays.

The total yield of photons is higher for annihilations than for decays since the flux $\Phi \sim \rho_\chi^2$ for annihilations, while $\Phi \sim \rho_\chi$ for decays. This can be seen from the general expresssion for the differential photon flux in a solid angle region $\Delta\Omega$:

$$
\begin{aligned}
(\frac{d\Phi_\gamma}{dE_\gamma})_{annih}(\Delta\Omega, E_\gamma) &= \frac{1}{4\pi}\frac{\langle\sigma v\rangle}{2m_\chi^2}\sum_i b_i(\frac{dN_\gamma}{dE_\gamma})_i\,\bar{J}_{annih}\,\Delta\Omega \qquad (25)\\
(\frac{d\Phi_\gamma}{dE_\gamma})_{decay}(\Delta\Omega, E_\gamma) &= \frac{1}{4\pi}\frac{1}{m_\chi\,\tau_\chi}\sum_i b_i(\frac{dN_\gamma}{dE_\gamma})_i\,\bar{J}_{decay}\,\Delta\Omega\\
\bar{J}_{annih} = \frac{1}{\Delta\Omega}\int_{\Delta\Omega} d\Omega \int_{los} \rho_\chi^2(r(s))\,ds;&\quad \bar{J}_{decay} = \frac{1}{\Delta\Omega}\int_{\Delta\Omega} d\Omega \int_{los} \rho_\chi(r(s))\,ds
\end{aligned}
$$

Here, $\bar{J}_{annih}$ ($\bar{J}_{decay}$) corresponds to the integrated squared (linear) DM density profile along the line-of-sight, and $(\frac{dN_\gamma}{dE_\gamma})_i$ is the photon spectrum coming from DM annihilations or decays for channel i with branching ratio b_i. Because of the different parametric dependence on ρ_χ, $\left(\frac{\bar{J}_{decay}}{\rho_{solar}\,r_{solar}}\right) \ll \left(\frac{\bar{J}_{annih}}{\rho_{solar}^2\,r_{solar}}\right)$ especially for "steep" profiles like NFW, etc. This implies that the decay mode gives rise to a much weaker signal compared to that for the annihilation mode. On the other hand, the decay mode satisfies the existing constraints from various observations of gamma rays much more easily than the annihilation mode. Table IV B lists the values of $\bar{J}_{annih}$ and $\bar{J}_{decay}$ (normalized such that they are dimensionless) for the GC for two qualitatively different profiles - the NFW and Isothermal profiles.

	$\frac{\bar{J}^2_{annih}}{\rho^2_{solar}\,r_{solar}}$	$\frac{\bar{J}_{decay}}{\rho_{solar}\,r_{solar}}$
NFW	$\approx 15\times 10^3$	≈ 28.9
Isothermal	≈ 13	≈ 5.7

TABLE I: $\bar{J}_{annih}$ and $\bar{J}_{decay}$ for the NFW and Isothermal profiles of the GC in the Milky Way for standard choices of astrophysical parameters, as in [12, 15].

Since the decay modes give rise to a much weaker signal, we will only show results for the annihilation mode, the one in (16) in particular. All three sources mentioned above will contribute to the total photon yield for our framework in general. For photon energies $E_\gamma \lesssim 100$ GeV, the contribution from ICS turns out to be the most important [7]. For $E_\gamma \gtrsim 100$ GeV, the contribution from π^0 decay takes

over and dominates over the ICS and FSR contributions. However, since the quantitative predictions for $E_\gamma \lesssim 100$ GeV are subject to various uncertainties in the ICS signal from astrophysics, we do not attempt to analyze the above energy regime in this work. Having said that, GLAST/FERMI is expected to be quite sensitive in this energy range [32]. So, a strong signal by GLAST/FERMI will provide very strong evidence for significant high energy electron (positron) production in the GC.

For $E_\gamma \gtrsim 100$ GeV, one can study the detectability of photon fluxes from DM annihilations or decays in Cerenkov detector based experiments such as VERITAS 4 which is expected to have a very high sensitivity in this energy range. The differential flux sensitivity of VERITAS 4 is expected to be $\sim 8 \cdot 10^{-4} - \sim 2 \cdot 10^{-5}\,\mathrm{GeVcm^{-2}s^{-1}sr^{-1}}$ in the energy range 100-1000 GeV [32]. The top plot of Figure 3 shows the predictions for the photon intensity for the annihilation mode in the 100-1000 GeV range, where π^0 decays dominate the photon yield. From the figure, it can be seen that future experiments like VERITAS 4 have a very good potential of detecting these very high energy gamma rays in the annihilation mode, particularly for steeper profiles like NFW. However, steep profiles may lead to some tension with the flux observed by EGRET in the energy range 10-100 GeV. HESS has also made observations of gamma rays coming from the GC [33] and the Galactic Ridge (GR) [34]. However, these observations are not ideal for DM observations because of the large contamination from gamma ray point sources as well as from molecular gas which are not well known. In addition, the effective $\bar{J}_{annih}$ relevant for these experiments is smaller because one has to subtract "off-source" contributions [16]. So, we do not attempt to analyze constraints from these observations although one could presumably still place some conservative bounds.

Another set of important constraints for $E_\gamma \gtrsim 100$ GeV comes from HESS observations the dwarf spheroidal galaxy (dSph) Sagittarius [35] which is believed to have negligible foregrounds, and hence is suitable for DM observations. Observations of other nearby galaxies from MAGIC, CANGAROO and WHIPPLE give similar constraints, so we will just study the constraints from HESS. HESS reports an upper bound on the integrated gamma ray flux $\Phi_\gamma^{max} = 3.6 \times 10^{-12}\,\mathrm{cm^{-2}\,s^{-1}}$ for $E_\gamma > 250$ GeV [35]. From this, the following upper bounds on the DM annihilation cross-section (decay width) can be derived:

$$\begin{aligned} \langle \sigma\, v \rangle_{max} &= \left(\frac{8\pi \Phi_\gamma^{max}\, m_\chi^2}{\bar{J}_{annih} \Delta\Omega\, \bar{N}_\gamma}\right);\ \Gamma_{max} = \left(\frac{4\pi \Phi_\gamma^{max}\, m_\chi}{\bar{J}_{decay} \Delta\Omega\, \bar{N}_\gamma}\right) \\ \text{where } \bar{N}_\gamma &= \left(\int_{250\,\mathrm{GeV}}^{m_\chi} \frac{dN_\gamma}{dE_\gamma}\, dE_\gamma\right) \end{aligned} \tag{26}$$

where $\Delta\Omega = 2 \times 10^{-5}$ is the HESS solid angle region. The quantity $\bar{N}_\gamma$ in (26), *viz.* the number of photons above ~ 250 GeV, can be estimated from the differential photon spectrum, as in [36]. At present, there is considerable amount of uncertainty in the DM density profile, which can vary from a cusped profile (with various allowed values of the cusps) to cored power-law profiles (with various values of the power-law exponent). We will look at two qualitatively different profiles, a large-core profile and an NFW profile, whose $\bar{J}$ (normalized such that they are dimensionless) values are listed in Table IV B. As for the GC, one finds that $\left(\frac{\bar{J}_{decay}}{\rho_{solar}\, r_{solar}}\right) \ll \left(\frac{\bar{J}_{annih}}{\rho_{solar}^2\, r_{solar}}\right)$. Therefore, we will only study the constraints for the annihilation mode in (16).

The bottom plot of Figure 3 shows the upper bound on B_{tot}^γ as a function of m_χ for the NFW and Large-Core profiles of Sagittarius in the annihilation mode (16). The area below the curves is consistent with the HESS observations of Sagittarius. A correct interpretation of these constraints requires some

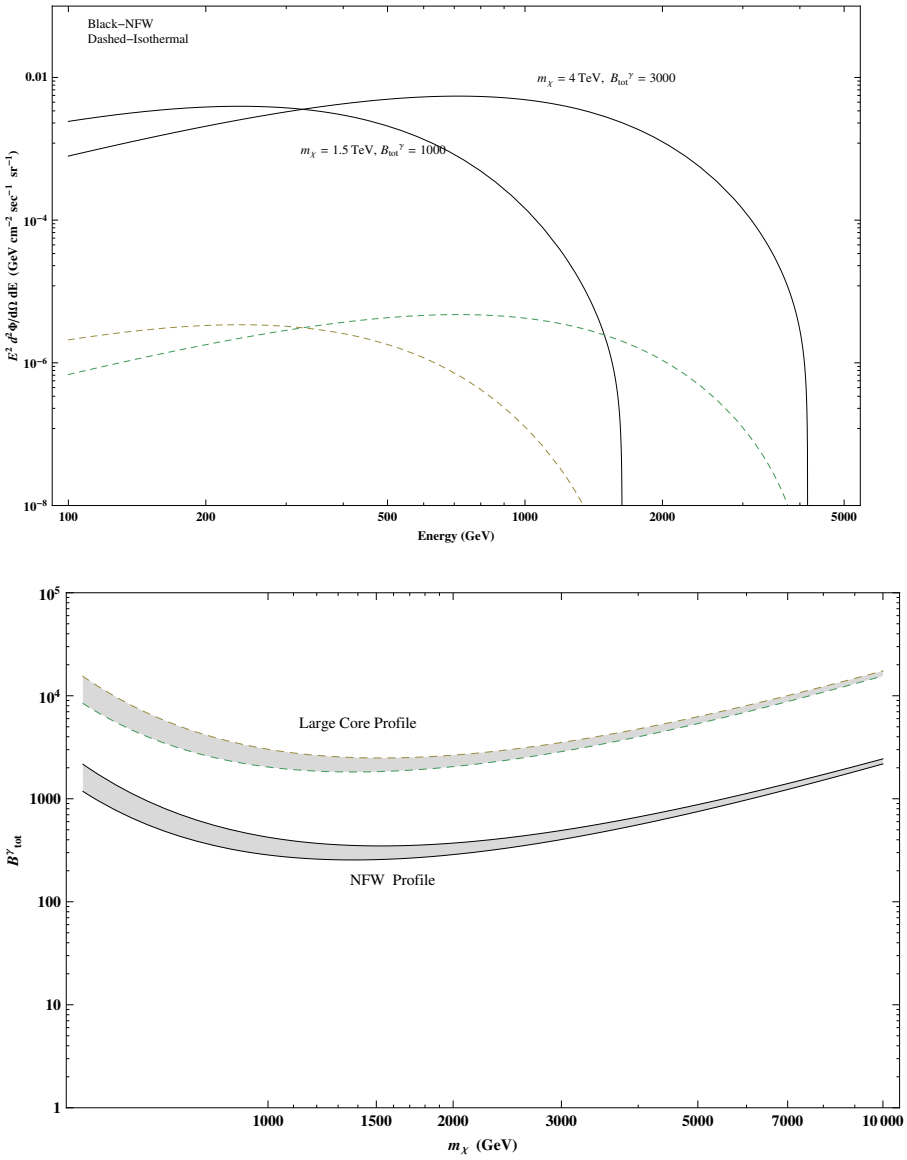

FIG. 3: **Top**: The photon intensity spectrum from the Galactic Center in the annihilation mode (16) for DM masses $m_\chi = 1.5$ TeV ($B^\gamma_{tot} = 1000$) and $m_\chi = 4$ TeV ($B^\gamma_{tot} = 3000$) with $m_H, m_A = 100$ GeV. The black curves stand for the NFW profile while the dashed curves stand for the Isothermal profile. The boost factor for photons B^γ_{tot} is explained below (27). **Bottom**: Upper bound on B^γ_{tot}, as computed in (26), as a function of m_χ for the annihilation mode (16). The black curves stand for the NFW profile while the dashed curves stand for the Large-Core profile of Sagittarius. The parametrization in [36] for $\frac{dN_\gamma}{dx}$ is used. The shaded area corresponds to the uncertainty in extracting the photon spectrum $\frac{dN_\gamma}{dx}$ from Monte-carlo simulations.

explanation. Taking into account the possible enhancements in the signal from (26), one finds that the boost factor for photons is given by:

$$B^\gamma_{tot} = B_{\sigma v} \cdot B^\gamma_{clump} \cdot B_{\rho_0} = B^e_{tot} * (\frac{B^\gamma_{clump}}{B^e_{clump}\, B_{\tau_E}}) \tag{27}$$

	$\frac{\bar{J}_{annih}}{\rho^2_{solar}\, r_{solar}}$	$\frac{J_{decay}}{\rho_{solar}\, r_{solar}}$
NFW	$\approx 1 \times 10^3$	$\approx 1.3 \times 10^{-4}$
Large Core	$\approx 1.4 \times 10^2$	$\approx 1.2 \times 10^{-5}$

TABLE II: $\bar{J}_{annih}$ and $\bar{J}_{decay}$ for the NFW and Large-core profiles of the Sagittarius dwarf spheroidal galaxy for standard choices of astrophysical parameters, as in [12, 15].

where we have used (22). In general, the boost factors arising from clumpiness in the halo is different for electrons (positrons) and photons. This is because electrons and positrons observed at the earth come from a short distance (since they lose energy very quickly) whereas photons can come from very far away. This implies that B^e_{clump} is close to the *local* clumpiness boost factor B^{local}_{clump} while B^γ_{clump} strongly depends on the direction of the gamma-ray source relative to the earth [37]. So, B^γ_{clump} could be smaller than from B^e_{clump} by a factor around 1-10. Together with an uncertainty of a factor of two in B_{τ_E}, this could give rise to B^γ_{tot} consistent with the bounds set by HESS. Note that the precise value of B^e_{tot} required to explain the PAMELA and ATIC data can itself be changed by optimizing over the astrophysical parameters consistent with the uncertainties. We have utilized the discrepancy between B^γ_{clump} and B^e_{clump} and the uncertainty in B_{τ_E} in the top plot of Figure 3, and have taken B^γ_{tot} as 1000 and 3000 for $m_\chi = 1.5$ TeV and 4 TeV respectively[5]. On the other hand, if B^γ_{clump} is not sufficiently smaller than B^e_{clump}, this would give rise to a tension between the parameters required for explaining PAMELA and ATIC (in the annihilation mode (16)) and the bounds set by the HESS observations of Sagittarius. This tension is more severe for the case of an NFW profile of Sagittarius (a little more than an order of magnitude) .

To summarize, observations of gamma-rays from the Sagittarius dwarf galaxy by HESS may provide strong constraints for the annihilation mode (16), primarily depending on the ratio of clumpiness boost factors B^γ_{clump} (in the Sagittarius direction) and B^e_{clump}. On the other hand, the decay modes in (18) and (19) can easily satisfy these bounds. As is obvious, the situation is reversed as far as prospects for future signals are concerned. The annihilation modes (16) and (17) can give rise to observable signals from the GC, which could be measured by VERITAS 4.

C. Neutrinos

A DM candidate which annihilates or decays to μ's or τ's will also give rise to a significant flux of neutrinos and can provide non-trivial constraints. It was noted in [17, 18] that the neutrino flux from the direction of the Galactic Center (GC) provides constraints for both annihilation and decay modes, with constraints for annihilation modes being much stronger (especially for steeper DM profiles). The neutrinos coming from the direction of the GC can be observed by detecting the muon flux induced by these neutrinos. A detector in the northern hemisphere (such as Super-Kamiokande) can detect upward going muons produced by neutrinos from the GC. One has to take into account that the three flavors of neutrinos oscillate into one another while traveling through the galaxy. As was pointed out in [38],

[5] These turn out to lie in between the upper bounds set for the NFW and Large Core profiles, as seen in the bottom plot of Figure 3.

the observed neutrino-induced muon flux is almost independent of m_χ for annihilations (for fixed DM couplings, and small m_χ). This is because both the neutrino-nucleon cross-section and the muon range scale like energy while the DM annihilation signal is proportional to $1/m_\chi^2$. Thus, in contrast to the photon flux (see (25)), the neutrino-induced muon flux is proportional to the normalized second moment of the neutrino energy spectrum, i.e. $\frac{d\Phi_\mu}{dE} \propto (\frac{E}{m_\chi})^2 \frac{dN_{\nu_i}}{dE}$. For decays, a similar argument implies that the flux is proportional to m_χ. For heavier DM masses, the neutrino-nucleon cross-section grows less steeply as well as the energy loss term for muons starts becoming important, implying that the energetic muon flux is relatively suppressed [16]. It is also important to note that the neutrino flux from the direction of the GC is much less sensitive to the uncertainties in the DM profile, especially if one looks at the GC over a large-size cone centered at the GC. Then a large fraction of the total DM annihilation signal is contained within the observed region. Therefore, it is better to look at bounds set by Super-K for large-size cones ($\sim 10^\circ - \sim 30^\circ$) around the GC for robust results.

It was shown in [18] that the neutrino-induced muon flux from direct DM annihilation to $\tau^+\tau^-$ for $m_\chi \approx 2$ TeV, and $B^\nu_{tot} \approx 4500$ and an NFW profile which provides a good fit to the PAMELA and ATIC data, is slightly above the upper bound set by Super-K [39] for a cone-size of about 10° around the GC. When the DM annihilates via higgs messengers to $\tau^+\tau^-$, the neutrinos are softer than in the previous case. However, since the electrons (positrons) are also softer, explaining the ATIC data requires that the DM mass in this framework is quite heavy (≈ 4 TeV for the annihilation mode) with a large boost factor B^e_{tot} (≈ 10000). This effect tends to compensate the effect of soft neutrinos mentioned above [16] and one expects to get approximately the same neutrino flux as for the direct annihilation case[6]. This naively implies that the neutrino-induced muon flux for the annihilation mode (16) with an NFW profile of the GC is also above the bound set by Super-K. However, as for gamma-rays, one has to keep in mind that $B^\nu_{tot} \neq B^e_{tot}$ in general. The clumpiness boost factor B^ν_{clump} is similar to that for photons because neutrinos, like photons, hardly lose energy and come from far away. Therefore, B^ν_{clump} is strongly direction-dependent in general. To get more precise constraints from neutrinos coming from the direction of the GC, one has to know the ratio of B^ν_{clump} (in the direction of the GC)[7] and B^e_{tot}. As for photons, the results for the annihilation mode (16) for the isothermal profile and for all the decay modes (for most profiles) are within the bounds set by Super-K.

It is worth commenting about future experiments which are going to look at the neutrino flux coming from various sources. The Hyper-Kamiokande experiment, which is expected to have a sensitivity bigger than Super-Kamiokande by about two orders of magnitude, should be able to robustly detect a positive signal from DM annihilations (and even decays in many cases) to neutrinos through higgs messengers. For small cone-sizes ($\leq 2^\circ$), future experiments like ANTARES [40] and KM3neT [41] show exciting prospects for the framework. For example, ANTARES and KM3neT should be able to easily observe a significant neutrino signal from the GC for the annihilation modes in (16) and (17) for steep DM profiles (like NFW) because $\bar{J}_{annih}$ increases rapidly for small cone-sizes. The prospects for the decay modes are not as promising since $\bar{J}_{decay}$ increases very slowly for small cone-sizes. For high-energy neutrinos ($\gtrsim$ TeV) arising within the framework, KM3neT may also be able to identify tau neutrinos which would greatly help in suppressing the atmospheric background since there are a lot fewer atmospheric tau neutrinos.

[6] This has to be confirmed by explicit analysis.

[7] It is expected that B^ν_{clump} (GC direction) $< B^e_{clump} \approx B^{local}_{clump}$ [37] which would help in relaxing the bounds.

ICE-CUBE [42] does not look toward the GC, but will instead look for a neutrino-induced muon flux arising from DM annihilation or decays of DM particles which accrete in the earth and in the sun. [43] has studied the prospects for such a flux for direct DM annihilations to neutrinos and also via annihilation to charged leptons such as taus. It was found that direct DM annihilation to monochromatic neutrinos has good prospects for ICE-CUBE. This implies that the production of neutrinos via cascade decays through higgs messengers, as for modes (16), (17), (18) and the second mode in (19), are also not promising. The first decay mode in (19), however, does lead to a monochromatic neutrino, so one would expect that this provides much better prospects. As seen from Figure (2) in [43], discovery is possible for monochromatic neutrinos if the enhancement factor in the annihilation cross-section compared to $\langle\sigma v\rangle_{std}$ is $B_{\sigma v} \gtrsim$ 100-1000 because then the earth reaches equilibrium by the present time. However, the difference in the leptonic higgs framework is that the monochromatic neutrino signal arises from the *decay* of DM particles rather than their annihilation. Since the denisty of DM particles inside the earth ρ_χ^{earth} is much larger than that in the galactic halo and since the flux in the decay mode scales as ρ_χ^{earth} in contrast to as $(\rho_\chi^{earth})^2$ for annihilations, the flux is greatly reduced [44] and hence does not provide good detection prospects at ICE-CUBE [8].

To summarize, observation of neutrinos originating from DM annihilations (or decays) in the future will be crucial in greatly strengthening the DM interpretation of the PAMELA and ATIC signals over conventional astrophysical sources like pulsars since those do not give rise to a large flux of neutrinos. The annihilation modes (16) and (17) provide stronger constraints, but also provide a greater potential for detectability in future experiments. Therefore, these deserve more detailed studies. It is interesting to note that within the decay mode, neutrinos provide a better opportunity for future detection of heavier DM compared to photons since for a given DM density profile and decay width, $\frac{d\Phi_\mu}{dE} \propto m_\chi$ for neutrinos which is not true for the case of cosmic-ray photons.

V. HIGGS PHYSICS - COLLIDER SIGNALS

We now move on to studying the Higgs sector in greater detail and potential signals for the LHC. In order to do that, it is important to study the higgs potential which is relevant for understanding the production and decay modes of the various higgs bosons. As mentioned earlier, we work within the framework of a CP-invariant two-higgs doublet model. After electroweak symmetry breaking, this gives rise to two CP-even higgs scalars h and H, a CP-odd higgs scalar A, and a charged higgs scalar H^+. The couplings of these scalars to fermions was already discussed in section III. In the following subsections, we first study the higgs potential within the framework of a leptonic higgs and then discuss signals at the LHC.

[8] This is true even if one assumes the "best-case" scenario that the earth has reached equilibrium at the present time due to a sufficiently large annihilation cross-section.

A. The Higgs Potential

As stated in section III, we consider a two higgs doublet model in which a symmetry forces one of the higgs doublets, H_l, to couple only to leptons, and the other higgs doublet, H_q, to couple only to quarks. A simple example of such a symmetry is a discrete Z_2 parity, P_l, under which H_l is odd, H_q is even, the left-handed leptons are odd, while the left-handed quarks and right-handed quarks and leptons are even. Such an assignment enforces the couplings mentioned above.

The most general CP-invariant two higgs doublet potential consistent with the above parity can be written as:

$$V = -\mu_q^2(H_q^\dagger H_q) + \mu_l^2(H_l^\dagger H_l) + \frac{1}{2}\lambda_1(H_q^\dagger H_q)^2 + \frac{1}{2}\lambda_2(H_l^\dagger H_l)^2 + \lambda_3(H_l^\dagger H_l)(H_q^\dagger H_q) + \lambda_4(H_l^\dagger H_q)(H_q^\dagger H_l) + (\frac{1}{2}\lambda_5(H_l^\dagger H_q)^2 + h.c.). \quad (28)$$

It is not fine tuned to have a vacuum where the vev of the H_l is smaller than that of H_q by, say, a factor of three. A larger hierarchy of vevs can be naturally obtained as follows. The above potential has an asymmetric phase where H_q acquires a vev $v = 174$ GeV while H_l has no vev. This phase of the two Higgs doublet potential was studied in [45] for the Inert Higgs Doublet model, where it was found that this phase has a parameter space of comparable size to the standard phase, and depends essentially on the sign of μ_l^2. Suppose one now introduces a small, soft, parity breaking interaction in the potential

$$\Delta V = -(\mu^2 H_q^\dagger H_l + h.c.). \quad (29)$$

Inserting the vev of H_q into this interaction generates a linear term in H_l, and therefore a vev for H_l proportional to the small symmetry breaking parameter μ^2, which can naturally be taken as small as desired. This will then guarantee that $\tan\beta$ and $\sin\alpha$ are suppressed, as required from the arguments in section III. It is convenient to parameterize the small parameter μ^2 as $\mu^2 \equiv 2\epsilon\, v^2$ for later use. It is also helpful to list the number of independent parameters. Equations (28) and (29) have eight parameters. However, electroweak symmetry breaking gives rise to one condition among these parameters, reducing the number of independent parameters to seven. These can be taken as $\{\lambda_1, \lambda_2, \lambda_3, \lambda_4, \lambda_5, \epsilon, t_\beta\}$. In the linear approximation for $\sin\alpha$ and $\tan\beta$ (valid since both are small), the physical higgs masses and the higgs mixing angle, $\sin\alpha$, can be computed in terms of these parameters as:

$$\begin{aligned} m_H^2 &\approx 2\,(\epsilon\, t_\beta^{-1})\, v^2;\ m_h^2 \approx 2(\lambda_1)\, v^2; \\ m_A^2 &\approx 2\,(\epsilon\, t_\beta^{-1} - \lambda_5)\, v^2;\ m_{H^\pm}^2 \approx 2(\epsilon\, t_\beta^{-1} - \frac{1}{2}(\lambda_4+\lambda_5))\, v^2; \\ s_\alpha &\approx t_\beta \frac{(\lambda_3+\lambda_4+\lambda_5-\epsilon\, t_\beta^{-1})}{(\lambda_1 - \epsilon\, t_\beta^{-1})} \end{aligned} \quad (30)$$

where $s_\alpha \equiv \sin\alpha$ and $t_\beta \equiv \tan\beta$, and α and β lie in the range $-\pi/2 \le \alpha \le \pi/2$; $0 \le \beta \le \frac{\pi}{2}$. For $\lambda_{1,2..,5} = \mathcal{O}(1)$, and $\mu^2 \equiv \epsilon\, v^2 \ll |\mu_l|^2 \sim |\mu_q|^2 \sim v^2$, the parameter $\epsilon = \mathcal{O}(1)\, t_\beta$. From (30), this implies that under these conditions all higgs masses are comparable to each other, up to factors of $\mathcal{O}(1)$. Also, depending on whether $(\epsilon\, t_\beta^{-1})$ is smaller or greater than λ_1, m_H could be lighter or heavier than m_h. As we will show below, various choices of these $\mathcal{O}(1)$ numbers, consistent with the constraints from LEP as reviewed at the end of section III, can lead to a rich phenomenology at the LHC.

B. Potential Signals at the LHC

The leptonic higgs has very interesting collider phenomenology, with distinctive signal characteristics that hold irrespective of the explicit DM model. If the ATIC data is confirmed, then in our scheme the mass of the dark matter is too large for it to be made at the LHC. Rather the LHC signals are encoded in the Higgs messengers, and cover a wide range of dark matter models. Although H_q and H_l mix, the mixing is required to be small from dark matter considerations, so that the characteristics of the leptonic higgs is kept intact. In particular, the couplings of the mass eigenstate higgs bosons are shown in (7). Since α and β are both necessarily small, the higgs associated with EWSB, h, has SM couplings to quarks but couplings to leptons that can be considerably larger or smaller than in the SM. In the leptonic Higgs sector, H, A and H^+ all have enhanced couplings to leptons and suppressed couplings to quarks. This pattern of couplings is quite unlike that of the MSSM where the fundamental distinction is between up and down/lepton couplings, rather than between up/down and lepton couplings. The Higgs sector is as rich as in the MSSM, and hence here we are only able to provide a limited survey of the interesting signals. We choose to highlight the decays of the neutral higgs bosons to pairs of τ leptons, as this is the most direct link between cosmic-ray and LHC signals. In particular, we consider each of the cases: $Z^* \to HA \to 4\tau$; $H, h \to 2\,\tau$ and $h \to 2A/2H \to 4\,\tau$, in some detail and also briefly mention other possible LHC higgs signals such as the 8τ signal and the charged higgs signal.

1. *The $Z^* \to HA \to \bar{\tau}\tau\bar{\tau}\tau$ Signal*

The LHC signal for $\bar{\tau}\tau\bar{\tau}\tau$ via HA production is particularly robust because the HA production cross section is insensitive to the mixing angles α and β, as they are both small, and H, A decay to $\tau\tau$ with branching ratios larger than about 0.9. The cross section for HA production at the LHC is dominated by s-channel Z exchange (Drell-Yan production)[47]. This is shown in Figure 4.

For example, with $m_H = 100$ GeV and $m_A = 80$ GeV the cross section is about 350 fb, while with $m_H = m_A = 160$ GeV, the cross section is about 50 fb. This is the same as the cross section for HA production in the decoupling limit of the MSSM. However, in the MSSM the $\bar{\tau}\tau$ branching ratio of H and A is never larger than 0.08, and is frequently significantly smaller, depleting the $\bar{\tau}\tau\bar{\tau}\tau$ signal by at least two orders of magnitude, whereas for the examples of H and A masses given above we expect about 10500 and 1500 $\bar{\tau}\tau\bar{\tau}\tau$ events (before imposing any cuts) with an integrated luminosity of 30 fb^{-1}. The main background for this signal is expected to be diboson (Z) production in which the Z's decay to $\bar{\tau}\tau$. Given that the signal is independent of the mixing angles α and β, and depends only on m_H and m_A, which we expect to be bounded by about $2M_W$ and $m_H + m_Z$ respectively from earlier cosiderations, it will be very important to study a realistic simulation of this signal with selection cuts and detector effects.

Before moving on, it is worth pointing out that the same Drell-Yan process will also lead to H^+H^- production with roughly the same cross-section; hence it could give rise to an observable signal with sufficient luminosity for the dominant $H^+ \to \tau^+\nu_\tau$ and $H^- \to \tau^-\nu_\tau$ channels. This suggests a completely different strategy to search for charged higgs bosons in contrast to that for the MSSM, which focusses on production of charged higgs boson production in association with top quarks and then studying their hadronic ($t\,\bar{b}$) and leptonic ($\tau^+\nu$) decay signatures.

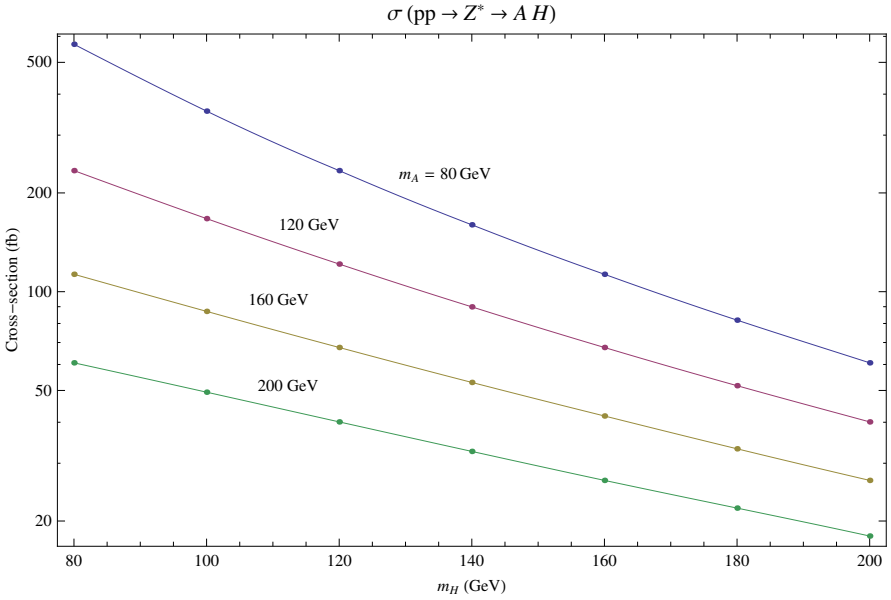

FIG. 4: Cross-section for $pp \to Z^* \to H\,A \to 4\tau$ as a function of m_H for different values of m_A at $\sqrt{s} = 14$ TeV, computed with CalcHEP [46].

2. *The $h, H \to \bar{\tau}\tau$ Signal*

The two τ signal from higgs decays has been studied in the SM. Although gluon fusion is the dominant production channel for the higgs, the search strategy for the $h_{SM} \to \bar{\tau}\tau$ mode consists of exploiting the vector boson fusion (VBF) channel for h_{SM} production, which has some distinct features that help to suppress the otherwise large backgrounds. Higgs production in this channel is usually accompanied by two jets in the forward region originating from the initial quarks from which vector bosons are emitted. Another feature is that no color is exchanged in the central hard process, leading to low jet activity in the central region. This is in contrast to most background processes. So, jet tagging in the forward region together with a veto of jet activity in the central region can help in achieving a high signal significance.

We estimate the $\sigma_{VBF} \times BR(\bar{\tau}\tau)$ for h and H, and compare it with the SM case for the same higgs mass. Since A does not couple to WW, one only has to consider h and H. One finds:

$$\sigma_{VBF}(h) \times BR(h \to \bar{\tau}\tau) \;\approx\; [\sigma^{SM}_{VBF} \times BR(h_{SM} \to \bar{\tau}\tau)]\, \frac{\left(\frac{\sin^2\alpha}{\sin^2\beta}\right)}{\left[1 + \left(\frac{\sin^2\alpha}{\sin^2\beta} - 1\right) BR(h_{SM} \to \bar{\tau}\tau)\right]} \qquad (31)$$

$$\sigma_{VBF}(H) \times BR(H \to \bar{\tau}\tau) \;\approx\; [\sigma^{SM}_{VBF} \times BR(h_{SM} \to \bar{\tau}\tau)]\, \frac{\sin^2(\alpha-\beta)}{BR(h_{SM} \to \bar{\tau}\tau)}.$$

For $m_H, m_h \lesssim 150$ GeV, the existing studies for the SM can be used to estimate the discovery potential in the proposed framework [48]. In these studies, the mode in which one of the τ's decays leptonically while the other decays hadronically is analyzed in detail for an integrated luminosity of $30\,fb^{-1}$. For this mode, $[\sigma^{SM}_{VBF} \times BR(h_{SM} \to \bar{\tau}\tau \to lj)]$, with $l = e/\mu$ and $j =$ jet, ranges between 45 and 155 fb for $145 > m_{h_{SM}} > 115$ GeV. After imposing various selection cuts to reduce the background, one gets

between ~ 4 to ~ 10 events for the signal, compared to about ~ 1.5 to ~ 3.5 events for the background [48]. This gives rise to a signal significance of about $3\sigma - 4\sigma$ for 30 fb^{-1} in the VBF production channel.

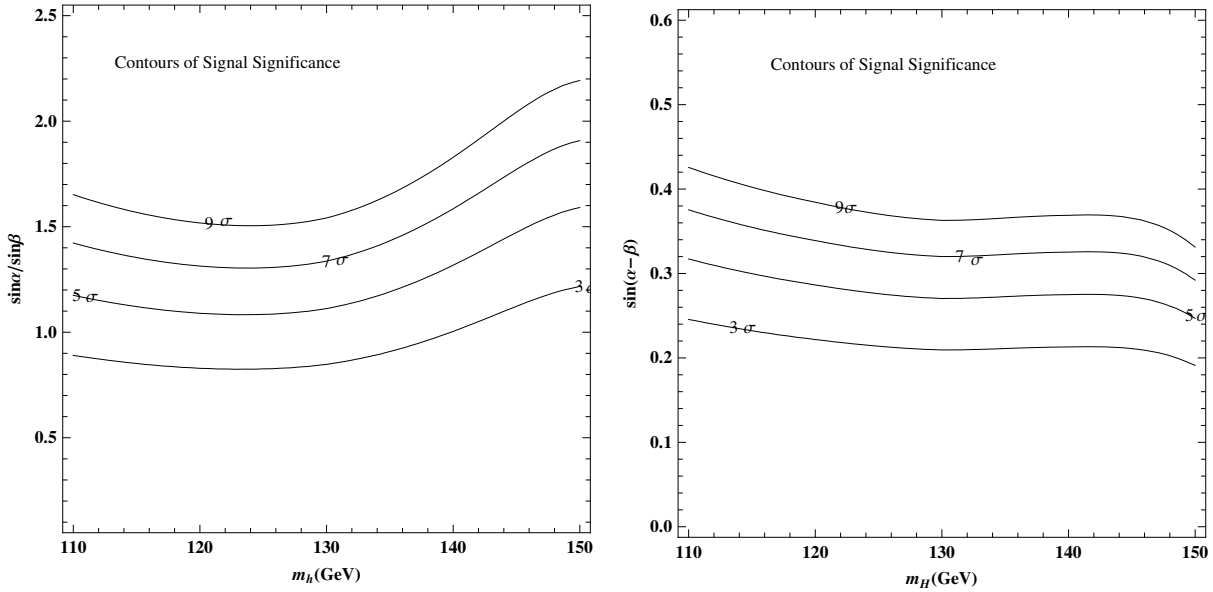

FIG. 5: Signal Significance contours for the $h \to \bar{\tau}\tau$ channel (**left**) and for the $H \to \bar{\tau}\tau$ channel (**right**) for an integrated luminosity of 30 fb^{-1}. Results from Figure 14 in [49] have been used.

For h and H, the signal is modified as in (31). First, we identify a parameter region that gives large signals for both h and H. A large value of $\sin\alpha$ relative to $\sin\beta$ is required, while both angles must be small to account for the DM signals. As a benchmark, one could take $\sin\alpha \approx \alpha = 0.35$ and $\sin\beta \approx \beta = 0.05$ giving rise to $\frac{\sin\alpha}{\sin\beta} \approx 7$, and $\sin(\alpha - \beta) \approx 0.3$. From (30), such a value of $\frac{\sin\alpha}{\sin\beta}$ can be obtained by choosing $\mathcal{O}(1)$ numbers for the λ's and ϵ. For the same range of masses for the higgses h, H as used for h_{SM} in [48], one finds for the benchmark values:

$$\begin{aligned} \sigma_{VBF}(h) \times BR(h \to \bar{\tau}\tau) &\approx (10-20)\,[\sigma^{SM}_{VBF} \times BR(h_{SM} \to \bar{\tau}\tau)] \\ \sigma_{VBF}(H) \times BR(H \to \bar{\tau}\tau) &\approx (1.1-3)\,[\sigma^{SM}_{VBF} \times BR(h_{SM} \to \bar{\tau}\tau)]. \end{aligned} \tag{32}$$

Thus, assuming that the results for the number of signal events scale in a simple way, one gets a huge signal significance of $\sim 40\,\sigma$ to $\sim 60\,\sigma$ for the h mode, and a significance of $\sim 4.4\sigma$ to $\sim 9\sigma$ for the H mode, for $115 < m_h, m_H < 145$ GeV in the VBF production channel for a luminosity of 30 fb^{-1}.

Of course, the benchmark values have been chosen to maximize the signal siginificance. To get a better idea of the allowed parameter space, in Figure 5 we show statistical significance contours in the $m_h - (\sin\alpha/\sin\beta)$ plane for h and in the $m_H - \sin(\alpha - \beta)$ plane for H. As long as $|\alpha| > \beta$ [9], while both are "small" ($|\alpha| \lesssim 0.3$), it seems reasonable to claim that the $\bar{\tau}\tau \to lj$ channel (especially for the h mode) provides an extremely robust signal and can be readily discovered at the LHC for higgs masses $\lesssim 150$ GeV. The above analysis is valid for $m_h, m_H \lesssim 2\,m_W$. For m_h much greater than $2\,m_W$, the $\bar{\tau}\tau \to lj$ channel does not seem promising as in this case h decays dominantly to WW and ZZ, which become the best modes to search for.

[9] β can always be chosen to lie in the first quadrant.

3. *The $h \to HH, AA \to \bar{\tau}\tau\bar{\tau}\tau$ Signal*

A 4τ signal is possible when $m_h > min\{2\,m_A, 2\,m_H\}$, with $h \to AA$ or HH and subsequent decays into four τ. The prospects for discovery through this mode are better when $m_h \lesssim 130$ GeV; otherwise the $t\bar{t}$ background becomes quite large and the branching ratio of $h \to A$ or H goes down as well. So, we will first analyze the case $130\,\mathrm{GeV} \gtrsim m_h > min\{2\,m_A, 2\,m_H\}$. The four τ final state is expected to have smaller background than the four b final state. Again, the most favored production channel is VBF for the same reasons as in the previous subsection. The higgs-strahlung production channel with leptonic gauge boson decay can also provide a nice trigger and better handle on the background. However, the cross section for this channel is much lower than that for VBF.

A full simulation study of the 4τ channel with the τ's decaying into $4\,\mu + 4\nu_\tau + 4\nu_\mu$ is currently under study at ATLAS [50] in the context of an NMSSM model in the VBF production channel of a SM-like higgs with the higgs decaying to AA followed by the decay to 4τ's, just as in the proposed framework. It requires three leptons to be observed and triggers on one or two high p_T leptons. CMS, on the other hand, is investigating the mode $4\,\tau \to \mu^\pm\mu^\pm\tau_{jet}^\mp\tau_{jet}^\mp$ containing two same sign muons and two τ jets in the context of the same NMSSM model framework [50]. Although a full study is currently unavailable, some studies of benchmark points in the NMSSM have been performed [51]. In these studies, the 4τ channel is studied when two τ's decay hadronically and the other two decay leptonically. For example, a benchmark NMSSM model, which seems to be quite similar to that for the proposed framework as far as the 4τ channel is concerned, is given by: $\{m_{h_1} = 120\,\mathrm{GeV}, m_{A_1} = 7\,\mathrm{GeV}, BR(h_1 \to A_1A_1) = 0.99, BR(A_1 \to \tau\tau) = 0.94\}$ where the h_1 behaves as a SM-like higgs as far as coupling to quarks and gauge bosons are concerned. A preliminary study of this benchmark model indicates that a signal significance of about 20 σ could be obtained for an integrated luminosity of $300\,fb^{-1}$ [51].

In the proposed framework, one has a similar situation as the above NMSSM benchmark model for the 4τ signal. The parameters m_h, $BR(h \to AA)$ and $BR(A \to \tau\tau)$ are very similar to their counterparts for the above NMSSM benchmark model for $m_h < 2\,m_W$. One possible exception is the mass of A which could be much heavier than that for the NMSSM model while still being consistent with a significant 4τ signal. For $m_h = 120$ GeV, one expects to get a similar statistical significance ($\sim 20\,\sigma$) as in the above benchmark model for 300 fb^{-1}. Since the proposed framework can have much heavier m_A, the two τ's from the decay of A are better separated implying that one could presumably get a better significance by utilizing this feature. If the signal and background are assumed to scale in a simple way, this would imply a statistical significance greater than 5 σ even for a luminosity of 30 fb^{-1}. Therefore, for $m_h \lesssim 130$ GeV, the 4τ channel may be used to make a discovery.

For heavier h, i.e. for $m_h \gtrsim 130$ GeV, the above search strategy is not as promising because of the huge $t\bar{t}$ background, which begins to rise sharply at about $M_{\tau\tau\tau\tau} = 140$ GeV [51]. Further studies from ATLAS and CMS are therefore needed to claim any significance for $m_h \gtrsim 130$ GeV. Finally, it is worth mentioning that in addition to studies at ATLAS and CMS, there is a study based on the proposed forward proton detector at the LHC, the so-called FP420 project [52]. This proposal utilizes the diffractive production $pp \to pph$ and detects protons in the final state. The claim from this study is that the final state basically consists of events with no backgrounds, implying that the masses of h and A can be determined on an event-by-event basis.

Finally, we would like to point out an interesting possibility arising from h pair-production. If $m_h >$

$min\{2\,m_A, 2\,m_H\}$ as above, h pair-production could lead to a spectacular 8 τ signal at the LHC. Higgs pair-production in the SM is dominated by gluon fusion [53]. For example, for a 120 GeV higgs (h_{SM}), the cross-section for h_{SM} pair-production is about 35 fb. The cross-section for h pair production in our framework is the same as that for the SM. This implies that one could get about 1000 8τ signal events (before imposing any cuts) for 30 fb^{-1}. Again, a detailed analysis of this channel would be quite interesting.

VI. SOME SIMPLE DM MODELS WITH LEPTONIC HIGGS

We now complete the picture in Figure 1 by explicitly constructing the DM sector and the couplings of this sector through the leptonic Higgs. To demonstrate the idea, we study three models: the $L - L^c - N$ model where the DM particle is Majorana fermion, and models where the DM particle is a scalar, either singlet or electroweak doublet. In each of these models, we consider both annihilation and decay modes.

A. $L - L^c - N$ DM Model

The dark sector in this model consists of a vector-like pair of lepton doublets L, L^c and a sterile neutrino N. L has exactly the gauge charges of the lepton doublet in the SM. The model has two Z_2 parities - a chiral lepton parity P_l introduced in section V A under which H_l and all the lepton doublets L, L^c and L_i are odd while all other fields are even, and a dark parity P_D under which only particles in the dark sector, L, L^c and N, are odd and all other particles are even. P_D guarantees that the lightest particle among L, L^c and N is stable and can be a dark matter candidate if it is neutral.

This model is similar to the model proposed in [54] except that it has an additional higgs which couples predominantly to leptons. The gauge couplings of L and L^c are standard, and the other renormalizable interactions involving the dark sector are:

$$\Delta\mathcal{L} \;=\; \eta_1 H_l^\dagger L N + \eta_2 H_l^T L^c N + m_L L L^c + \frac{1}{2} m_N\, N^2 \tag{33}$$

The nature of the DM candidate depends on the spectrum of the dark sector which in turn is determined by the mass parameters m_L, m_N and the higgs vev $\langle H_l \rangle = v_l$. The charged components $\chi^\pm$ in L and L^c form a Dirac fermion with mass m_L. N and the neutral components of L and L^c mix after electroweak symmetry breaking. The three neutral Majorana mass eigenstates (χ_1, χ_2, χ_3) and their corresponding masses (m_1, m_2, m_3), are given by:

$$\begin{pmatrix} \chi_3 \\ \chi_2 \\ \chi_1 \end{pmatrix} \sim \begin{pmatrix} 1 & \frac{(\eta_1-\eta_2)v_l}{\sqrt{2}(m_N+m_L)} & \frac{(\eta_1+\eta_2)v_l}{\sqrt{2}(m_N-m_L)} \\ O(v_l/m_N) & 1 & \frac{(\eta_1^2-\eta_2^2)v_l^2}{4m_L(m_N+m_L)} \\ O(v_l/m_N) & -\frac{(\eta_1^2-\eta_2^2)v_l^2}{4m_L(m_N-m_L)} & 1 \end{pmatrix} \begin{pmatrix} N \\ (L-L^c)/\sqrt{2} \\ (L+L^c)/\sqrt{2} \end{pmatrix} \tag{34}$$

$$\begin{aligned} m_3 &\sim m_N + O(v_l^2/m_N) \\ m_2 &\sim m_L + \frac{(\eta_1-\eta_2)^2}{2(m_N+m_L)} v_l^2 \\ m_1 &\sim m_L - \frac{(\eta_1+\eta_2)^2}{2(m_N-m_L)} v_l^2 \end{aligned} \tag{35}$$

If $m_N > m_L$, the spectrum becomes:

$$m_{\chi_1} < m_{\chi^\pm} < m_{\chi_2} < m_{\chi_3} \tag{36}$$

and one gets doublet dark matter. The splitting due to electroweak symmetry breaking guarantees that the lightest P_D odd particle is always neutral, and the splitting between χ_1 and χ_2 allows the model to evade the bound from direct detection by suppressing elastic scattering through coupling to a Z boson[10].

On the other hand, if $m_N < m_L$ one gets:

$$m_{\chi_3} < m_{\chi_1} < m_{\chi^\pm} < m_{\chi_2} \tag{37}$$

and one gets singlet dark matter. Therefore, this model allows the DM particle to be either a singlet or electroweak doublet. It is also possible to have decaying dark matter in this model if the dark parity P_D is broken by a small amount. We now discuss both DM annihilations and decays within this model. For simplicity, we assume that only one of the modes is responsible for the cosmic-ray signals although in principle it is possible that both modes are comparable.

1. Annihilating Dark Matter

The phenomenological consequences in the annihilation mode for singlet and doublet DM are different. In addition to the differences in the cross-section, a doublet DM particle has an unsuppressed coupling to the Z boson in contrast to a singlet one which doesn't couple to the Z. For singlet DM, it turns out that the dominant annihilation channel in the s-wave is $\chi\chi \to H\,A$ by a t-channel exchange of the heavier neutral partner of L and L^c. All other s-wave channels, such as ZZ, WW, Z-higgs, W-higgs, and fermion pairs ($f\bar{f}$) are suppressed because of the tiny mixing between the doublet and singlet components. The H^+H^-, HH and AA channels are also suppressed due to CP invariance. For doublet DM however, in addition to the $\chi\chi \to H\,A$ channel as before, annihilation to ZZ is also potentially relevant because of the unsuppressed coupling mentioned above. Since Z has a large hadronic branching ratio, the branching ratio of the doublet DM annihilating to ZZ has to be much smaller than that to $H\,A$ in order for it to be phenomenologically viable. The annihilation cross-sections for doublet DM are given by:

$$\begin{aligned} \sigma\, v^{(D)}\,(\chi\chi \to HA)_s &= \frac{(\eta_2^2-\eta_1^2)^2}{16\pi\, m_N^2 (1+\frac{m_L^2}{m_N^2})^2}(1+O(\frac{m_{H,A}^2}{2m_L^2})) \\ \sigma\, v^{(D)}\,(\chi\chi \to ZZ)_s &= \frac{g^4}{32\pi\cos^4\theta_W\, m_L^2}\,(1+O(\frac{m_Z^2}{m_L^2})) \end{aligned}$$

[10] Elastic scattering through the higgs is also suppressed due to the suppressed couplings of the leptonic higgs to quarks.

From the argument above, this implies a lower bound on the coupling $(\eta_2^2 - \eta_1^2)$ (for a given m_χ and $m_{\chi'}$). We know from section IV that in order to fit the PAMELA and ATIC data, the DM mass m_χ is required to be around 4 TeV and the total boost factor for positrons (electrons) B^e_{tot} needs to be around 10^4. Taking into account the local fluctuation of the DM density and other uncertainties which could naturally give rise to a boost factor of about 10, this would imply an enhancement of about 10^3 from the cross-section itself. For the doublet case, this naively implies that $\eta_2^2 - \eta_1^2 \sim 40$. However, it turns out that there is a mild Sommerfeld enhancement in this model due to formation of a wimponium bound state by W-exchange. This enhances the cross-section by a factor of about 10 if the mass splitting between χ_1 and χ^+ is less than 0.1 GeV [13]. From eq.(35), this small mass splitting can be achieved with $v_l < 5$ GeV corresponding to $\sin\beta \sim 3 \times 10^{-2}$ ($y_\tau \sim 0.3$). Therefore, a perturbative cross-section (38) which is smaller than that naively required (without the Sommerfeld enhancement) by a factor ~ 10 is also allowed. This in turn implies that a much smaller $\eta_2^2 - \eta_1^2$ is needed. For example, $\eta_1 << \eta_2 \sim 3.5$ can explain the PAMELA and ATIC data.

Moving on to the singlet case, the annihilation cross-section to $H\,A$ is given by:

$$\sigma\, v^{(S)}\,(\chi\chi \to H\,A)_s = \frac{(m_H^2 - m_A^2)^2}{4 m_N^2 m_L^2} \sigma\, v^{(D)}\,(\chi\chi \to H\,A)_s$$

This is suppressed compared to that for the doublet case by typically a factor of 10^{-4}, which would require the yukawa couplings η_1, η_2 to be much larger than the strong coupling limit to explain the observed data. Therefore, we do not discuss this case.

2. Decaying Dark Matter

It is interesting to consider this model in the decay mode since the annihilation mode is subject to more stringent constraints from cosmic-ray photons and neutrinos as explained in section IV. In order to have decaying DM in this model, the following P_D breaking terms can be added to the Lagrangian (33) consistent with all gauge symmetries:

$$\Delta\mathcal{L}_{decay} \;=\; \delta_{1i} H_l^\dagger L_i N + \delta_{2i} H_l^T L e_i^c + \delta_{3i} H_l^\dagger L^c e_i^c + \delta_i' m_L L_i L^c + h.c. \tag{38}$$

δ's are required to be extremely small to allow the DM lifetime to be around 10^{25-26} seconds. The particular form of the above interaction and the smallness of δ's can be explained by symmetry arguments in several different ways.

The mass mixing term in (38) with coefficient δ_i' dominates the decay process. Therefore, the parity P_l has to be suitably extended to give rise to sufficiently long decay lifetimes. One simple possibility is to extend P_l to the full chiral leptonic parity $P_{l_l} \times P_{l_r}$ where H_l is odd under both, L_i and N are odd under only P_{l_l}, while e_i^c, L and L^c are odd under only P_{l_r}. Then, the leading non-renormalizable operators are:

$$\frac{\phi_l \phi_r \phi_D}{M_{UV}^3}(c_{1i} H_l^\dagger L_i N + c_{2i} H_l^T L e_i^c + c_{3i} H_l^\dagger L^c e_i^c) + c_{4i} \frac{\phi_l \phi_r \phi_D}{M_{UV}^2} L_i L^c \tag{39}$$

where ϕ_l, ϕ_r and ϕ_D are scalar fields that are odd under P_{l_l}, P_{l_r} and P_D respectively, and are assumed to get *vevs* of order the electroweak scale, leading to:

$$\delta_i' \sim c_{4i} \frac{v^3}{M_{UV}^2 m_L}; \;\; \delta_{ij} \sim c_{ij} \frac{v^3}{M_{UV}^3} \tag{40}$$

δ' values with the correct magnitude are naturally obtained for $M_{UV} \approx M_{GUT}$. For singlet DM $\chi \approx N$, the dominant decay is through the yukawa couplings in (33) in which N decays to a leptonic higgs and the dark doublet L, L^c followed by the decay of L, L^c by mixing with the SM leptons L_i through the mixing term in (38). Thus, the decay modes in this case are given by:

$$\begin{aligned} \chi &\rightarrow (A, H) + \nu_l \rightarrow \tau^+\tau^-\nu_l \\ &\textit{or} \\ \chi &\rightarrow H^\pm + l^\mp \rightarrow \tau^\pm l^\mp \nu_\tau \end{aligned} \tag{41}$$

where $l = e, \mu, \tau$. This leads to different predictions for the electron and positron spectra for different l. As discussed in section IV A, this channel will give a different fit from both 4τ and 2τ cases. In general, the spectra is expected to be a *weighted* average of the 4τ, 2τ, 2μ and $2e$ cases depending on the relative weight of channels with different l. This will change the fit to PAMELA and ATIC and also the predictions for photon and neutrino fluxes. We leave the detailed study of this case for future work.

If the DM particle is a doublet, its dominant decay mode is by mixing with the SM lepton doublet L_i. There is no constraint from any flavor experiments since the operators are suppressed by the GUT scale. So all SM leptons L_i are equally likely to mix with the dark doublet. The possible decay channels in this case are $\chi \rightarrow Z\nu_i$, $W^\pm l^\mp$, $H_l^\pm \tau^\mp$. Since the vector boson channels are not only not suppressed by $\tan\beta$ but also enhanced by $(m_\chi/m_W)^2$ for heavy DM (due to dominant longitudinal mode couplings at high energies), these channels always dominate even for very small $\tan\beta$ (corresponding to $y_\tau \approx 1$). This case is close to the model recently proposed in [9]. However, since this case does not fit in our original framework of the DM sector coupling to the visible sector through a leptonic higgs, we do not discuss this case in section IV.

Finally, in order to suppress terms like:

$$\mathcal{L} \supset (H_q^\dagger L_i N + H_q^T L e_i^c) \tag{42}$$

which makes the DM particles decay dominantly to $l\bar{q}q$, we also assume that there is a quark parity P_q in the quark-H_q sector. If P_q is exact, this operator is completely forbidden. However, the μ^2 term in the potential (29) breaks P_q. In order to simultaneously generate the μ^2 term and suppress the above operator in a consistent way, we have to break the parity spontaneously by $\sim$ electroweak scale vevs. One way to do this is by introducing a scalar ϕ_q that is odd under P_q and P_{l_l}. So the above operator is suppressed by $\frac{\phi_l \phi_q \phi_D}{M_{UV}^3}$ and is suppressed compared to the dominant decay mode (the fourth term) in (38). μ^2 of the correct magnitude is generated if $\mu^2 = \epsilon \langle\phi_r\rangle\langle\phi_q\rangle$, where ϵ is a technically natural small coefficient.

B. Singlet Scalar DM Model

A particularly simple form of dark matter is a singlet complex scalar field Φ. The couplings of Φ to the SM is trivially constrained to the higgs sector, the extended higgs sector in our picture. With a discrete symmetry $\Phi \rightarrow -\Phi$, the most general addition to the scalar potential is

$$\Delta V \;=\; m_\Phi^2\, \Phi^\dagger\Phi + \lambda \Phi^\dagger\Phi (H_l^\dagger H_l + x H_q^\dagger H_q) + \lambda' (\Phi^\dagger\Phi)^2. \tag{43}$$

We assume the relative strength x of the quartic couplings to H_q and H_l is small, i.e. $x < 1/3$, so that dark matter annihilates dominantly via $H_l^\dagger H_l$ to 4 τ. Taking $m_\Phi = 4$ TeV, to allow for an explanation of the ATIC as well the PAMELA data, we find a galactic annihilation cross section relative to $\langle\sigma v\rangle_{std} = 3\times 10^{-26}\mathrm{cm}^3\mathrm{s}^{-1}$ by a factor $B_{\sigma v} \approx 50\, n^2 R$, where $\lambda = n\pi^2$ and R is the Sommerfeld enhancement factor. An attractive yukawa potential is generated between the annihilating Φ particles by the exchange of the scalars in both H_l and H_q, with a strength proportional to $\lambda^2 v_l^2$ and $x^2\lambda^2 v_q^2$, respectively. Since the dark matter particle is expected to be about 30 times heavier than the exchanged scalar, the resulting Sommerfeld enhancement factor can be significant. For example, $n = 4$, and either $x \sim 1/3$ or $v_l/v_q \sim 1/3$, leads to a region where R is rapidly varying from 10 to in excess of 100. Hence $B_{\sigma v}$ of order $10^3 - 10^4$, as required to explain PAMELA and ATIC, is possible, even for perturbative values of λ. As λ is increased, the one-loop radiative correction to the mass term $H_l^\dagger H_l$ also increases, leading to a little hierarchy problem of why the H and A states are significantly lighter than the dark matter Φ. This is a general naturalness problem for models with annihilation of heavy dark matter to leptonic Higgs states lighter than $2M_W$. The large coupling needed for a large annihilation cross section leads to a large radiative contribution to the leptonic Higgs mass parameter from a loop with internal dark matter particles.

We can also have a decaying scalar dark matter by introducing a Z_6 parity so that the leading interaction that couples Φ linearly to SM particles is the dimension 6 interaction

$$\Delta\mathcal{L} \;=\; \frac{1}{m_{UV}^2}\phi_D^3 \Phi H_l^\dagger H_l + h.c. \tag{44}$$

Under the Z_6 symmetry, $\Phi \to -\Phi$ and $\phi_D \to e^{i\frac{\pi}{3}}\phi_D$, while all SM particles transform trivially. Taking the scalar ϕ_D to acquire a weak scale vev, and taking m_{UV} of order 10^{16} GeV, leads to decays of Φ to 4τ with a lifetime of order 10^{26} seconds. This case would require m_χ to be around 8 TeV (see section IV).

C. Inert Higgs-Doublet DM Model

Finally, we consider the scalar DM to be an electroweak doublet. A simple example of this is the inert Higgs H_I, first proposed in [55]. Extending this model, we have three Higgs-doublets, H_q, H_l and H_I, where both H_q and H_l get a vev but the inert Higgs H_I does not. The Higgs doublets are all identical in the sense of gauge charges, but have different masses and parities. The couplings of H_I to fermions are forbidden by dark parity. Since no symmetry can forbid the term $(H_I^\dagger H_I)(H_q^\dagger H_q)$, we have no symmetry explanation of suppressing the couplings of H_I to the quark sector in this model. One can only claim that it is not unreasonable to have such couplings being numerically suppressed. However, such a possibility is at least naturally allowed within the framework of a leptonic higgs sector.

From now on, we concentrate on couplings to leptonic higgs. The relevant new terms in the scalar potential are:

$$\Delta V \;=\; m_I^2 H_I^\dagger H_I + H_I^\dagger H_I H_l^\dagger H_l - (H_I^\dagger H_l)(H_l^\dagger H_I) + (H_I^\dagger H_l)^2 + c.c. \tag{45}$$

We omit the $\mathcal{O}(1)$ coefficients in front of each quartic term to avoid use of new notation. These terms allow the lightest P_D odd particle to be neutral after electroweak symmetry breaking splits the doublet. The second quartic term splits the charged and neutral components of H_I, while the last term in (45) splits the scalar and the pseudoscalar parts of the neutral component in H_I, naturally evading bounds from

direct detection. The DM particles can annihilate to $H_l^\dagger H_l \to 4\tau$. However, similar to the doublet DM in the LL^cN model, the ZZ annihilation channel is also present. In order to fit the ATIC data we need some of these quartic couplings to be large and the mass splitting between the scalar and pseudoscalar (and charged and neutral) components to be small (to provide a modest Sommerfeld enhancement), requiring a hierarchy between these quartic couplings.

A decaying scalar dark matter is also possible by introducing small dark parity breaking term. Similar to the LL^cN model, the lowest dimensional operator is the mass mixing term:

$$\Delta\mathcal{L}_{decay} \;=\; \delta m^2 H_I^\dagger H_l + c.c. \tag{46}$$

The corresponding term involving the quark Higgs can be forbidden by imposing an exact quark parity as we did for the the LL^cN model. The desired small value for δm^2 can again be obtained by extending P_l to the full chiral lepton parity and the dark parity P_D to Z_4 in which H_I has 2 units of charge. Then, the parity preserving non-renormalizable operator is:

$$\Delta\mathcal{L}_{decay} \;=\; \frac{\phi_D^2 \phi_l \phi_r}{m_{UV}^2} H_I^\dagger H_l + c.c. \tag{47}$$

The parities of these ϕ's are as defined in the LL^cN model except the $\phi_D \to i\phi_D$ under the Z_4 discrete dark symmetry. The possible decay channels are WW, ZZ, $(A, H)\, h$, $\bar{\tau}\tau$ and the three-body decay to $(A, H)\, hh$. The vector boson channels are enhanced by $(m_\chi/m_W)^2$ as before but unlike the case for fermionic DM, these vector boson channels are also suppressed by $\sin^2\beta$. Therefore, the $\bar{\tau}\tau$ channel can dominate when $\sin\beta$ is relatively small. For example, for $\sin\beta \sim 10^{-2}$ ($y_\tau \sim 1$), the decay branching ratio to vector bosons is about 5% for 4 TeV dark matter. The scalar decay channels come from quartic interactions (for example $\lambda_3 |H_l|^2 |H_q|^2$) in the potential which can not be forbidden by any symmetry. However, the two-body decay mode is suppressed by at least $(v_q/M_\chi)^2 \sim 10^{-3}$ while the three-body decay mode is suppressed by an extra phase factor of $\sim 1/2\pi^2$. For quartic couplings not much bigger than unity, the $\bar{\tau}\tau$ channel can dominate the decay. Since the final state is $\bar{\tau}\tau$, a 4 TeV decaying dark matter of this model is expected to fit the data well.

VII. CONCLUSIONS AND SUMMARY

In this paper we have explored the consequences of assuming that a leptonic Higgs mediates the interactions between the dark matter sector and the Standard Model sector. The motivation for this approach is two-fold. One is theoretical: the same TeV mass scale underlies both the breaking of weak interactions and the dark matter annihilation rate, indicating a close connection between the dark matter and Higgs sectors. The observational motivation is that the cosmic ray signals are *leptonic*; in particular, the limits on a primary $\bar{p}$ flux indicate that mediation via a Higgs with quark couplings should be subdominant. We study the minimal case of a single leptonic Higgs, in which case its largest couplings to matter must be to τ leptons, with couplings to e and μ that are sufficiently small to play no role. The Higgs potential could lead to mass mixing between the states with leptonic and quark couplings but, again, the absence of an exotic primary cosmic ray $\bar{p}$ flux limits this mixing to be small. Hence, there is one neutral mass eigenstate scalar, H, one pseudoscalar, A, and one charged scalar H^+ that maintain their dominant leptonic couplings. This allows an important connection between the leptonic cosmic ray

signals and the expected Higgs signatures at the LHC. In both cases there are signals that arise from the production of H, A and H^+ and their subsequent decays to τ leptons. From LEP limits and the leptonic cosmic ray signals we argue that the states H, A and H^+ are likely to have masses in the range of roughly 100 GeV to 200 GeV.

The leptonic cosmic ray signals, for both PAMELA and ATIC, could arise from a variety of channels: dark matter annihilation to $\tau^4, \tau^2\nu^2$ or dark matter decay to $\tau^4, \tau^2, \tau^2\nu, \tau\nu l$ via intermediate H, A and H^+ states. For concreteness we have computed the cosmic ray signals for the case of annihilations $\chi\chi \to \tau^4$, and the results are shown in Figure 2. Good fits to the PAMELA and ATIC data can be simultaneously obtained for m_χ in the region around 4 TeV. We have also commented on all the other possible annihilation and decay modes. The width of the peak in the leptonic signal around 600 GeV is larger than in the case of annihilations or decays directly to e and μ, and we expect this to be a common feature of all modes involving τs. Similarly we expect the signal in the positron fraction to continue to energies larger than the present PAMELA data, and not to show a sharp peak. Such an annihilation signal requires a large total boost factor in the annihilation cross section of order 10^4, but essentially identical cosmic ray signals can result from dark matter decays with lifetimes of order 10^{26} seconds.

We have computed the photon spectrum that results from annihilations of DM via pairs of leptonic Higgs states to τ^4 in the dwarf galaxy Sagittarius. For a DM mass of 4 TeV, HESS data places a limit of $\sim 10^3$ ($\sim 10^4$) on the relevant boost factor, B^γ_{tot}, for the case that Sagittarius has an NFW (Large Core) profile. For this annihilation mode and DM mass, the PAMELA and ATIC signals require a boost factor B^e_{tot} that is of order 10^4. However, these two boost factors are not identical in general, so further observations of hard gamma rays from Sagittarius would provide a powerful probe of this annihilation channel. We also compute the high energy gamma ray signal expected from DM annihilations in the center of the Milky Way galaxy, as shown in the top plot of Figure 3, which could be detected by VERITAS 4. The annihilation channel to 4τ also produces a galactic flux of neutrinos which is in mild conflict with the bounds set by SuperK on upward going neutrinos through the Earth, if the relevant neutrino and electron boost factors are identical. As before, these boost factors can differ, so future neutrino measurements also offer the possibility of a crucial independent verification of the DM origin of the charged lepton cosmic ray signals. In addition, an observation of energetic cosmic neutrino flux strongly favors the dark matter interpretation of the cosmic-ray signals over astrophysical ones (such as pulsars) in general since astrophysical sources do not emit a large flux of high energy neutrinos.

For the decay modes, constraints from current gamma-ray and neutrino observations are easily satisfied but at the same time these also lead to less promising prospects for future experiments. For heavy decaying dark matter, neutrinos provide a better opportunity for future experiments compared to gamma rays, since the neutrino flux is proportional to the dark matter mass.

A common feaure of the cosmic ray signals discussed above is that the dark matter particle has a mass in excess of 1 TeV and is not expected to be produced at the LHC. While cosmic ray photon and neutrino fluxes allow discrimination between DM annihilation and decay, the LHC probes a completely complementary feature of the theory – the production and decay of the leptonic Higgs states H, A and H^+. There is a very rich and distinctive Higgs phenomenology; all the couplings of these states to matter and to electroweak gauge bosons are determined by just their masses and two mixing angles, as shown in (7). The τ^4 signal for $H\,A$ production via a virtual Z is particularly robust because it is insensitive to the values of the small Higgs mixing angle α and to the ratio of vevs $\tan\beta$. Depending on the H and A

masses this $H\,A$ production cross section is typically in the (50-250) fb region, and from the cosmic ray signals we know that the branching ratio to τ^4 is close to unity. Detailed simulation studies are needed to estimate the observability of this τ^4 signal.

We have computed $\sigma\times$BR for the production of both the leptonic Higgs scalar H and the Higgs boson h in the vector-boson (WW) fusion at the LHC followed by decay to τ pairs. For $m_H, m_h \lesssim 2M_W$, discovery at the LHC is possible for a wide range of α and β, provided $|\alpha| > \beta$, via the channel $\bar{\tau}\tau \to lj$, and for some regions of parameter space the signal is very large allowing prompt discovery at the LHC. If $m_h > 2m_H$ or $2m_A$ the τ^2 signal for h production is lost, but the cascade $h \to HH, AA \to \tau^4$ leads to a 4τ signal instead. Comparisons with benchmark studies for 4τ signals in the next-to-minimal supersymmetric theory suggest that a 5σ discovery may be possible with an integrated luminosity of 30 fb^{-1} for $m_h < 130$ GeV. Further simulation studies are needed, especially for $m_h > 130$ GeV where backgrounds from top quark pair production become important. Other LHC Higgs signals, such as charged higgs pair-production by Drell-Yan followed by their decay to $\tau^{\pm}\nu$, and a spectacular 8τ signal from h pair-production, are also possible and would be quite interesting to study further.

Simple particle physics models of DM that couples to the visible sector via a leptonic Higgs are very easy to write down. In the case that DM is a heavy lepton, the interaction with the leptonic Higgs is via a yukawa coupling, allowing s-wave annihilations to $H\,A$. On the other hand, scalar dark matter can annihilate via a quartic scalar interaction to H or A pairs. In either case a large annihilation cross section is possible, aided in many cases by a modest Sommerfeld boost factor; but in both cases the DM abundance must be produced non-thermally. Alternatively, the DM could be produced thermally, with the cosmic ray signals arising from decays. The long lifetime follows from a decay amplitude that is suppressed by two powers of the ratio of the weak scale to the unified scale, which arises from a combination of breaking the discrete symmetry that leads to near stability of the DM and the discrete symmetry that ensures the leptonic nature of the Higgs.

Acknowledgments

We would like to thank Yasunori Nomura, Alessandro Strumia and Jesse Thaler for useful discussions. HG would like to thank the KITPC for their hospitality where part of his research was conducted. This work is supported by the U.S. Department of Energy under contract no. DE-AC02- 05CH11231 and NSF grant PHY-04-57315 .

[1] O. Adriani *et al.*, arXiv:0810.4994 [astro-ph]; O. Adriani *et al.*, arXiv:0810.4995 [astro-ph].

[2] S. W. Barwick *et al.* [HEAT Collaboration], Astrophys. J. **482**, L191 (1997) [arXiv:astro-ph/9703192].

[3] M. Aguilar *et al.* [AMS-01 Collaboration], Phys. Lett. B **646**, 145 (2007) [arXiv:astro-ph/0703154].

[4] J. Chang *et al.*, Nature **456**, 362 (2008).

[5] S. Torii *et al.*, arXiv:0809.0760 [astro-ph].

[6] N. Arkani-Hamed, D. P. Finkbeiner, T. Slatyer and N. Weiner, arXiv:0810.0713 [hep-ph]; M. Pospelov and A. Ritz, Phys. Lett. B **671**, 391 (2009) [arXiv:0810.1502 [hep-ph]]; A. E. Nelson and C. Spitzer, arXiv:0810.5167 [hep-ph];Y. Nomura and J. Thaler, arXiv:0810.5397 [hep-ph]; P. J. Fox and E. Poppitz, arXiv:0811.0399 [hep-ph]; M. Fairbairn and J. Zupan, arXiv:0810.4147 [hep-ph]; Y. Bai and Z. Han, arXiv:0811.0387 [hep-

ph]; K. M. Zurek, arXiv:0811.4429 [hep-ph]; E. J. Chun and J. C. Park, arXiv:0812.0308 [hep-ph]; R. Allahverdi, B. Dutta, K. Richardson-McDaniel and Y. Santoso, arXiv:0812.2196 [hep-ph]; D. Hooper, A. Stebbins and K. M. Zurek, arXiv:0812.3202 [hep-ph]; C. R. Chen, K. Hamaguchi, M. M. Nojiri, F. Takahashi and S. Torii, arXiv:0812.4200 [astro-ph]; I. Gogoladze, R. Khalid, Q. Shafi and H. Yuksel, arXiv:0901.0923 [hep-ph]; D. E. Kaplan, M. A. Luty and K. M. Zurek, arXiv:0901.4117 [hep-ph]; P. Grajek, G. Kane, D. J. Phalen, A. Pierce and S. Watson, arXiv:0807.1508 [hep-ph]; D. Feldman, Z. Liu and P. Nath, arXiv:0810.5762 [hep-ph]; S. C. Park and J. Shu, arXiv:0901.0720 [hep-ph]; J. H. Huh, J. E. Kim and B. Kyae, arXiv:0809.2601 [hep-ph]; K. J. Bae, J. H. Huh, J. E. Kim, B. Kyae and R. D. Viollier, arXiv:0812.3511 [hep-ph]; X. J. Bi, P. H. Gu, T. Li and X. Zhang, arXiv:0901.0176 [hep-ph].

[7] I. Cholis, G. Dobler, D. P. Finkbeiner, L. Goodenough and N. Weiner, arXiv:0811.3641 [astro-ph]; I. Cholis, L. Goodenough and N. Weiner, arXiv:0802.2922 [astro-ph]; I. Cholis, D. P. Finkbeiner, L. Goodenough and N. Weiner, arXiv:0810.5344 [astro-ph].

[8] R. Harnik and G. D. Kribs, arXiv:0810.5557 [hep-ph].

[9] D. J. Phalen, A. Pierce and N. Weiner, arXiv:0901.3165 [hep-ph].

[10] C. R. Chen, F. Takahashi and T. T. Yanagida, arXiv:0811.0477 [hep-ph]; C. R. Chen, M. M. Nojiri, F. Takahashi and T. T. Yanagida, arXiv:0811.3357 [astro-ph]; K. Hamaguchi, S. Shirai and T. T. Yanagida, arXiv:0812.2374 [hep-ph]; P. f. Yin, Q. Yuan, J. Liu, J. Zhang, X. j. Bi and S. h. Zhu, arXiv:0811.0176 [hep-ph]; K. Ishiwata, S. Matsumoto and T. Moroi, arXiv:0811.4492 [astro-ph]; K. Ishiwata, S. Matsumoto and T. Moroi, arXiv:0811.0250 [hep-ph]; F. Takahashi and E. Komatsu, arXiv:0901.1915 [astro-ph]; A. Arvanitaki, S. Dimopoulos, S. Dubovsky, P. W. Graham, R. Harnik and S. Rajendran, arXiv:0812.2075 [hep-ph]; B. Kyae, arXiv:0902.0071 [hep-ph].

[11] A. Ibarra and D. Tran, arXiv:0811.1555 [hep-ph].

[12] E. Nardi, F. Sannino and A. Strumia, arXiv:0811.4153 [hep-ph].

[13] J. Hisano, S. Matsumoto, M. M. Nojiri and O. Saito, Phys. Rev. D **71**, 063528 (2005) [arXiv:hep-ph/0412403]; J. D. March-Russell and S. M. West, arXiv:0812.0559 [astro-ph].

[14] N. F. Bell and T. D. Jacques, arXiv:0811.0821 [astro-ph]; L. Bergstrom, G. Bertone, T. Bringmann, J. Edsjo and M. Taoso, arXiv:0812.3895 [astro-ph].

[15] G. Bertone, M. Cirelli, A. Strumia and M. Taoso, arXiv:0811.3744 [astro-ph].

[16] J. Mardon, Y. Nomura, D. Stolarski and J. Thaler, arXiv:0901.2926 [hep-ph].

[17] J. Hisano, M. Kawasaki, K. Kohri and K. Nakayama, arXiv:0812.0219 [hep-ph].

[18] J. Liu, P. f. Yin and S. h. Zhu, arXiv:0812.0964 [astro-ph].

[19] V. Silveira and A. Zee, Phys. Lett. B **161**, 136 (1985).

[20] J. March-Russell, S. M. West, D. Cumberbatch and D. Hooper, JHEP **0807**, 058 (2008) [arXiv:0801.3440 [hep-ph]].

[21] M. Cirelli, M. Kadastik, M. Raidal and A. Strumia, arXiv:0809.2409 [hep-ph].

[22] F. Donato, D. Maurin, P. Brun, T. Delahaye and P. Salati, arXiv:0810.5292 [astro-ph].

[23] P. Grajek, G. Kane, D. Phalen, A. Pierce and S. Watson, arXiv:0812.4555 [hep-ph].

[24] V. D. Barger, J. L. Hewett and R. J. N. Phillips, Phys. Rev. D **41**, 3421 (1990); Y. Grossman, Nucl. Phys. B **426**, 355 (1994) [arXiv:hep-ph/9401311]; A. G. Akeroyd, Phys. Lett. B **377**, 95 (1996) [arXiv:hep-ph/9603445]; A. G. Akeroyd, J. Phys. G **24**, 1983 (1998) [arXiv:hep-ph/9803324]; R. A. Porto and A. Zee, Phys. Lett. B **666**, 491 (2008) [arXiv:0712.0448 [hep-ph]]; R. A. Porto and A. Zee, Phys. Rev. D **79**, 013003 (2009) [arXiv:0807.0612 [hep-ph]]; M. Aoki, S. Kanemura and O. Seto, arXiv:0807.0361 [hep-ph]; Talk by Shufang Su, http://online.kitp.ucsb.edu/online/lhc_c08/su/ ; Talk by Brooks Thomas, http://agenda.hep.wisc.edu/getFile.py/access?contribId=140&sessionId=27&resId=0&materialId=2&confId=60

[25] T. Moroi and L. Randall, Nucl. Phys. B **570**, 455 (2000) [arXiv:hep-ph/9906527]; B. S. Acharya, P. Kumar, K. Bobkov, G. Kane, J. Shao and S. Watson, JHEP **0806**, 064 (2008) [arXiv:0804.0863 [hep-ph]]; P. Kumar, arXiv:0809.2610 [hep-ph].

[26] S. Schael *et al.* [ALEPH Collaboration and DELPHI Collaboration and L3 Collaboration and], Eur. Phys. J. C **47**, 547 (2006) [arXiv:hep-ex/0602042].

[27] A. Heister *et al.* [ALEPH Collaboration], Phys. Lett. B **543**, 1 (2002) [arXiv:hep-ex/0207054].

[28] J. Olzem, H. Gast and S. Schael, Nucl. Phys. Proc. Suppl. **173**, 51 (2007).

[29] C. Amsler *et al.* [Particle Data Group], Phys. Lett. B **667**, 1 (2008).

[30] T. Delahaye, R. Lineros, F. Donato, N. Fornengo and P. Salati, Phys. Rev. D **77**, 063527 (2008) [arXiv:0712.2312 [astro-ph]]; T. Delahaye, F. Donato, N. Fornengo, J. Lavalle, R. Lineros, P. Salati and R. Taillet, arXiv:0809.5268 [astro-ph].

[31] J. Lavalle, Q. Yuan, D. Maurin and X. J. Bi, arXiv:0709.3634 [astro-ph].

[32] T.C. Weekes, Talk Given at UCLA.
`http://gamma1.astro.ucla.edu/future_cherenkov/Talks/weekes_ucla.ppt`

[33] F. Aharonian *et al.* [H.E.S.S. Collaboration], Phys. Rev. Lett. **97**, 221102 (2006) [Erratum-ibid. **97**, 249901 (2006)] [arXiv:astro-ph/0610509].

[34] F. Aharonian *et al.* [H.E.S.S. Collaboration], Nature **439**, 695 (2006) [arXiv:astro-ph/0603021].

[35] F. Aharonian et al [HESS Collaboration], Astropart. Phys. **29**, 55 (2008) [arXiv:0711.2369 [astro-ph]].

[36] N. Fornengo, L. Pieri and S. Scopel, Phys. Rev. D **70**, 103529 (2004) [arXiv:hep-ph/0407342].

[37] http://www.umich.edu∼mctp/SciPrgPgs/events/2009/LHC/talks/090108-Edsjo-indirect-uncert-opt.pdf

[38] S. Ritz and D. Seckel, Nucl. Phys. B **304**, 877 (1988).

[39] S. Desai *et al.* [Super-Kamiokande Collaboration], Phys. Rev. D **70**, 083523 (2004) [Erratum-ibid. D **70**, 109901 (2004)] [arXiv:hep-ex/0404025].

[40] T. Stolarczyk [ANTARES Collaboration], Nucl. Phys. Proc. Suppl. **165**, 188 (2007).

[41] J. Carr *et al.* [KM3NeT Collaboration], arXiv:0711.2145 [astro-ph].

[42] J. Ahrens *et al.* [IceCube Collaboration], Astropart. Phys. **20**, 507 (2004) [arXiv:astro-ph/0305196].

[43] C. Delaunay, P. J. Fox and G. Perez, arXiv:0812.3331 [hep-ph].

[44] K. Griest and D. Seckel, Nucl. Phys. B **283**, 681 (1987) [Erratum-ibid. B **296**, 1034 (1988)].

[45] R. Barbieri, L. J. Hall and V. S. Rychkov, Phys. Rev. D **74**, 015007 (2006) [arXiv:hep-ph/0603188].

[46] A. Pukhov *et al.*, arXiv:hep-ph/9908288; A. Pukhov, arXiv:hep-ph/0412191.

[47] S. Dawson, S. Dittmaier and M. Spira, Phys. Rev. D **58**, 115012 (1998) [arXiv:hep-ph/9805244].

[48] G.L. Bayatiyan *et al.* [CMS Collaboration], J. Phys. G: Nucl. Part. Phys. 34 (2007) 9951579

[49] S. Abdullin *et al.*, Eur. Phys. J. C **39S2**, 41 (2005).

[50] N. E. Adam *et al.*, arXiv:0803.1154 [hep-ph].

[51] K. A. Assamagan *et al.* [Higgs Working Group Collaboration], arXiv:hep-ph/0406152.

[52] J. R. Forshaw, J. F. Gunion, L. Hodgkinson, A. Papaefstathiou and A. D. Pilkington, JHEP **0804**, 090 (2008) [arXiv:0712.3510 [hep-ph]].

[53] F. Gianotti *et al.*, Eur. Phys. J. C **39**, 293 (2005) [arXiv:hep-ph/0204087].

[54] R. Enberg, P. J. Fox, L. J. Hall, A. Y. Papaioannou and M. Papucci, JHEP **0711**, 014 (2007) [arXiv:0706.0918 [hep-ph]]; R. Mahbubani and L. Senatore, Phys. Rev. D **73**, 043510 (2006) [arXiv:hep-ph/0510064]; F. D'Eramo, Phys. Rev. D **76**, 083522 (2007) [arXiv:0705.4493 [hep-ph]].

[55] R. Barbieri, L. J. Hall and V. S. Rychkov, Phys. Rev. D **74**, 015007 (2006) [arXiv:hep-ph/0603188].